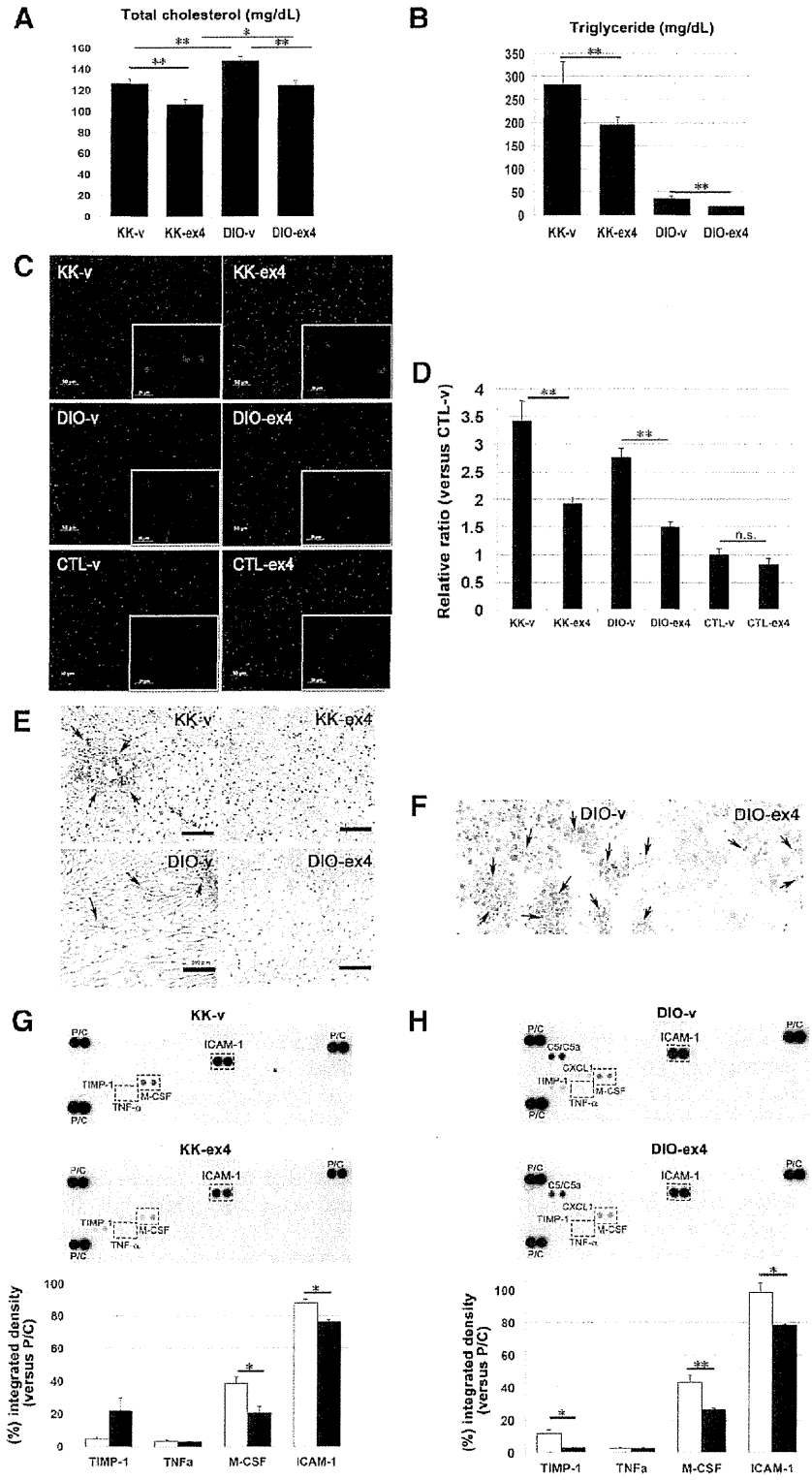

Fig. 5. Effect of Ex-4 on systemic and cardiac lipid levels and inflammatory cytokines. Effect of Ex-4 on plasma cholesterol (*A*) and triglyceride (*B*) levels. Ex-4 decreased both total cholesterol and triglyceride levels in KK and DIO groups. *C*: effect of Ex-4 on cardiac steatosis. Changes in cardiac steatosis were detected by ceramide staining (red). Both KK-v (*left, top*) and DIO-v (*left, middle*) exhibited higher lipid accumulation in the heart, which was reversed by Ex-4 treatment (*right, top* and *middle*). Scale bar = 50 μm (inset: 20 mm). Data were converted to densitometric value and summarized as a relative ratio vs. CTL-v (*D*). $^{**}P <$ 0.01 vs. CTL-v (n = 7–10). *E* and *F*: lipid accumulation observed in myocardium (*E*) and liver (*F*). In myocardium, Oil-red-O staining revealed the lipid accumulation (arrow); however, its pattern was patchy and the number of positive spots was much less than the case observed in liver. Ex-4 reduced the Oil-red-positive spots both in myocardium and liver as previously reported. *G* and *H*: screening for Ex-4-sensitive inflammatory cytokine(s) using cytokine array. Representative blots obtained by specimen of KK (*G*) and DIO (*H*) were displayed. Data were summarized by densitometry (white bar, vehicle control; and black bar, Ex-4-treated group). Ex-4 partially but significantly reduced intercellular adhesion molecule-1 (ICAM-1) and macrophage colony-stimulating factor (M-CSF). Regarding tumor necrosis factor-α (TNF-α), it remained unchanged and likewise with other positively detected molecule: tissue inhibitor of metalloproteinase-1 (TIMP-1), complement 5/5a (C5/C5a), and chemokine (C-X-C motif) ligand 1 (CXCL1). P/C, positive control of each array. $^{**}P < 0.01$ and $^{*}P <$ 0.05 vs. vehicle counterpart.

remodeling; however, it remains unclear whether therapeutic intervention for metabolic disorder may reverse these relevant cardiac remodeling. GLP-1, one of the incretine hormones, has been focused not only as an alternative therapeutic target for diabetes but also for its pleiotropic effects on cardiovascular disease, including heart failure related to pacing-induced heart failure (22), myocardial infarction (23), and obesity (24).

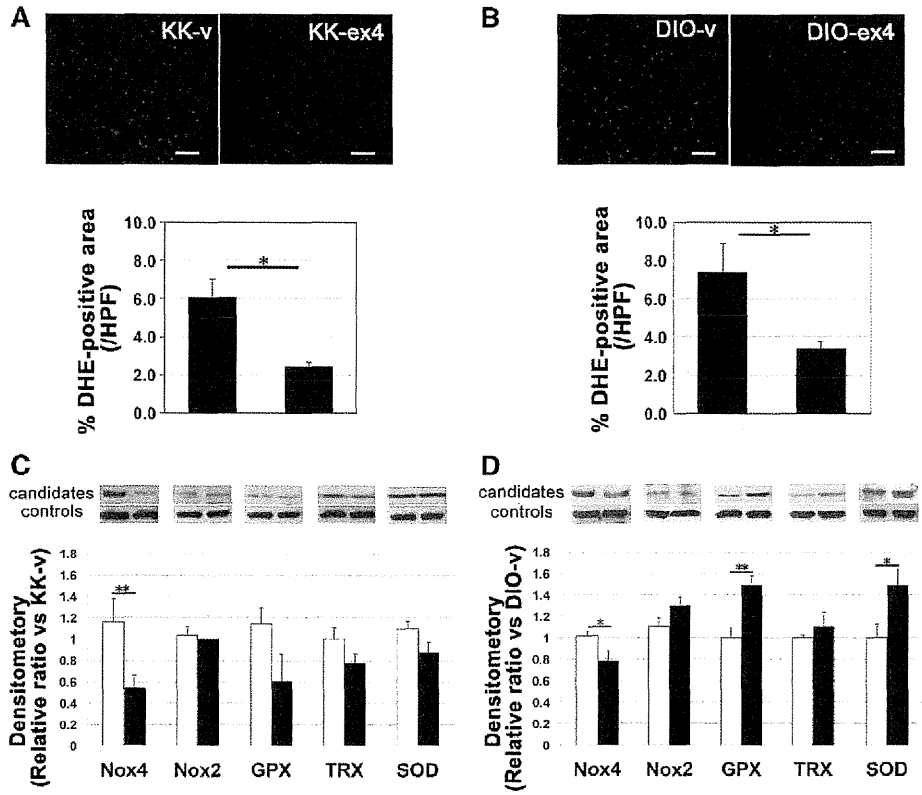

Fig. 6. Effect of Ex-4 treatment on cardiac oxidative stress. *A* and *B*: impact of Ex-4 on cardiac oxidative stress level detected by fluorescence dye dihydroethidium (DHE; red spots). Ex-4 reduced cardiac oxidative stress both in KK (*A*) and DIO (*B*). The DHE-positive area was quantified as a percentage in each total HPF (magnification, ×200) area. $*P < 0.05$ (n = 7–10). Scale bar = 50 μm. *C* and *D*: changes in oxidative stress-related molecules. Representative immunoblots displayed as a pair of reactive oxygen species-related molecules (candidates, *top*) as follows: NADPH oxidases (Nox: Nox2, Nox4), GPX glutathione peroxide (GPX), thioredoxine (TRX), and superoxide dismutase-1 (SOD). Each band was measured by densitometry and summarized in each graph represented below the representative images. White bar, vehicle-treated type 2 diabetes mellitus (T2DM) mice; black bar: Ex-4 treated. $**P < 0.01$; $*P < 0.05$ (n = 7–10).

Primary findings of the present study are as follows: *1*) GLP-1R agonist Ex-4 ameliorates cardiac remodeling and dysfunction observed in T2DM independently of etiology with concomitant amelioration of systemic and cardiac insulin resistance (Figs. 2–4); *2*) Ex-4 reduced circulating cholesterol levels (Fig. 5, *A* and *B*) and cardiac steatosis (Fig. 5, *C–E*); *3*) Ex-4 reduced circulating inflammatory cytokines, in particular, ICAM-1 and M-CSF (Fig. 5, *G* and *H*); *4*) Ex-4 reduced cardiac oxidative stress by reversing the levels of Nox-4 (KK and DIO) and antioxidant molecules (exclusively to DIO) (Fig. 6).

Recently, Noyan-Ashraf et al. (24) have reported the same trend regarding the impact of GLP-1-receptor analog on the obesity-induced cardiac dysfunction under distinct experimental conditions from those applied in the present study. Liraglutide, the protease-resistant analog of GLP-1, ameliorates cardiac dysfunction via improving cardiac inflammation and corresponding ER stress response, leading to improved cardiac dysfunction in animals on HFD by an AMP-activated protein kinase-dependent mechanism. They concluded that liraglutide had no effect on the of mitochondrial biogenesis and respiration by selected evaluation of those marker protein levels (PGC-1α, cytochrome *c*, and cytochrome-*c* oxidase subunit IV); however, their study did not demonstrate any change in mitochondrial remodeling as well as inflammatory cytokine/ROS target screening. Growing evidence demonstrates that ROS links to inflammation, and, in particular, mitochondria-derived ROS could provoke the upregulation of inflammatory cytokines (21), suggesting the underlying mechanisms of the GLP-1 axis-mediated amelioration of cardiac function could be explained at least two pathway by amelioration of cardiac mitochondrial remodeling by reducing cardiac ROS and inflammation as presented in the present study (Fig. 7) and by ER stress demonstrated by Noyan-Ashraf et al. (24).

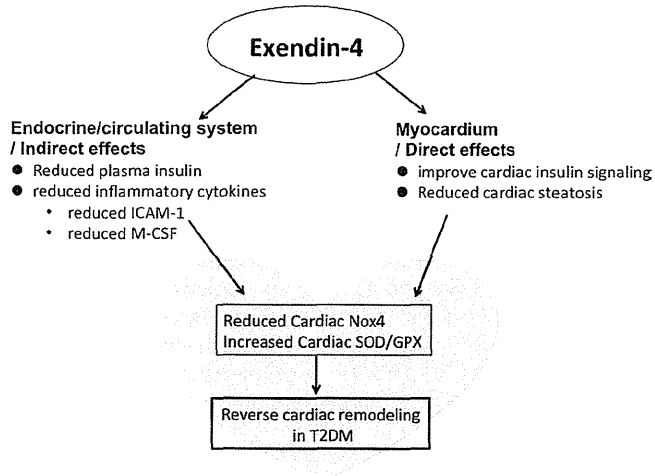

Fig. 7. Suggested mechanisms underlying the reversal effects of glucagon-like peptide-1 receptor activation on cardiac remodeling induced by type 2 diabetes. Overnutrition triggers dyslipidemia leading to abnormal lipid loading, which results in cardiac steatosis and insulin resistance presumably via inflammation and oxidative stress. Enhanced insulin resistance and lipotoxicity induced by cardiac steatosis promote enhanced oxidative stress that destroys mitochondrial integrity. Glucagon-like peptide-1 receptor activation counteracts these overnutrition-mediated dyslipidemia, cardiac steatosis, and cardiac insulin resistance.

We demonstrated that Ex-4 ameliorated systemic and cardiac insulin resistance (Fig. 2). Of note, cardiac insulin resistance links to ROS-mediated mitochondrial dysfunction (6). The Ex-4-mediated mitigation of impaired cardiac insulin signaling may also contribute to the reverse remodeling of diabetic myocardium. In addition, it is noteworthy that Nox-4 is presumably responsible for the Ex-4-mediated reduction of ROS (Fig. 6, *C* and *D*). It is noteworthy that Nox-4 is essential to insulin signal propagation (17) and cardiac remodeling (16, 18). Interestingly, Nox-4 signaling links to ICAM-1, which is an inflammatory mediator that also increases in T2DM (9) and selectively decreased by Ex-4 (Fig. 5, *G* and *H*) (27), suggesting that the essential effects of Ex-4 may be mediated by ICAM-1/Nox-4 axis. Exclusively in DIO group, we found concomitant increase in antioxidant molecules, namely SOD-1 and GPx (Fig. 6*D*). It remains ambiguous why Ex-4 had no effect on the antioxidant molecules in KK heart, which could be speculated because of the difference in genetic background, suggesting some caution regarding choosing model(s) when analyze the oxidative stress in T2DM.

M-CSF was found to be another Ex-4-sensitive cytokine in the present study (Fig. 5, *G* and *H*). M-CSF is a lineage-specific cytokine that promotes the survival, proliferation, and differentiation of mononuclear phagocytes (30), and, of note, its receptor increased collagen deposition within the myocardial infarct area (38), suggesting the M-CSF pathway might contribute to the generation in cardiac fibrosis that occurred in diabetic myocardium (Fig. 3, *C* and *D*), which could be another mechanism underlying the GLP-1R agonism-mediated reverse remodeling in diabetic myocardium. Future evaluation is desirable.

A study limitation of the present study is considered as follows: we had no data regarding the molecular mechanism how GLP-1 agonism may reverse cardiac steatosis. Excess lipid accumulation to non-adipocyte cells arises in the setting of dyslipidemia or lipid overload resulted from mismatch of lipid supply and consumption (31). This pathological lipid overload promotes lipotoxicity leading to pathological remodeling and dysfunction in local tissue. Indeed, the present study (Fig. 5, *A* and *B*) and previous data (20) demonstrated that GLP-1R activators mitigate dyslipidemia. When we consider the case of hepatic steatosis, this excellent study has been demonstrated that GLP-1 agonism markedly decreased hepatic content of cholesterols and phospholipids, accompanied by downregulation of hepatic lipogenesis-related genes and ApoB synthesis (26). Furthermore, it is also considerable that Ex-4 may modulate "cardiac" peroxisome proliferator-activated receptor-γ (PPAR-γ) because Ex-4 increases hepatic PPAR-γ expression in rat (34). PPAR-γ is primarily a regulator of lipid storage and transport in adipocytes and macrophages, and it elicits transdifferentiation of fibro- and myoblasts into adipocytes (11), suggesting the Ex-4 may reverse cardiac steatosis via modulating cardiac PPAR-γ axis. In addition to cardiomyocyte, Goto et al. (8) recently demonstrated that capillary endothelial PPAR-γ in heart promotes fatty acid uptake by heart in the postprandial state after long-term fasting. Taken together, the role of GLP-1R/PPAR-γ axis in cardiac steatosis seems unignorable, and future study is awaited.

In summary, the present study comprehensively demonstrated the advantage of therapeutic intervention for diabetic myocardial remodeling by exploring the GLP-1 axis-mediated molecular mechanisms.

ACKNOWLEDGMENTS

We thank Ikuyo Mizuguchi and Yoshikazu Fujita at the Division of Medical Research Engineering, Nagoya University Graduate School of Medicine, for technical support.

Present address of T. Shigeta: Div. of Cardiology, Gifu-prefectural Tajimi Hospital, 5-161, Maehata-cho, Tajimi, Gifu, 507-8522, Japan.

GRANTS

This work was supported in part by Ministry of Education, Culture, Sports, Science, and Technology Japan Grants-in-Aid for Scientific Research 20249045 and 23390208 (to T. Murohara) and 23591080 (to Y. K. Bando) and by the Suzuken Memorial Foundation (to Y. K. Bando).

DISCLOSURES

No conflicts of interest, financial or otherwise, are declared by the author(s).

AUTHOR CONTRIBUTIONS

A.M., T. Mitsui, M.A., and T.S. performed experiments; A.M., T. Mitsui, Y.K.B., and M.A. analyzed data; A.M. and Y.K.B. interpreted results of experiments; A.M., T. Mitsui, and Y.K.B. prepared figures; A.M. and Y.K.B. drafted manuscript; A.M., T. Mitsui, Y.K.B., M.A., T.S., and T. Murohara approved final version of manuscript; Y.K.B. conception and design of research; T. Murohara edited and revised manuscript.

REFERENCES

1. **Aguirre V, Werner ED, Giraud J, Lee YH, Shoelson SE, White MF.** Phosphorylation of Ser307 in insulin receptor substrate-1 blocks interactions with the insulin receptor and inhibits insulin action. *J Biol Chem* 277: 1531–1537, 2002.
2. **Ban K, Noyan-Ashraf MH, Hoefer J, Bolz SS, Drucker DJ, Husain M.** Cardioprotective and vasodilatory actions of glucagon-like peptide 1 receptor are mediated through both glucagon-like peptide 1 receptor-dependent and -independent pathways. *Circulation* 117: 2340–2350, 2008.
3. **Best JH, Hoogwerf BJ, Herman WH, Pelletier EM, Smith DB, Wenten M, Hussein MA.** Risk of cardiovascular disease events in patients with type 2 diabetes prescribed the glucagon-like peptide 1 (GLP-1) receptor agonist exenatide twice daily or other glucose-lowering therapies: a retrospective analysis of the LifeLink database. *Diabetes Care* 34: 90–95, 2011.
4. **Best JH, Lavillotti K, DeYoung MB, Garrison LP.** The effects of exenatide bid on metabolic control, medication use and hospitalization in patients with type 2 diabetes mellitus in clinical practice: a systematic review. *Diabetes Obes Metab* 14: 387–398, 2012.
5. **Boudina S, Abel ED.** Diabetic cardiomyopathy revisited. *Circulation* 115: 3213–3223, 2007.
6. **Boudina S, Bugger H, Sena S, O'Neill BT, Zaha VG, Ilkun O, Wright JJ, Mazumder PK, Palfreyman E, Tidwell TJ, Theobald H, Khalimonchuk O, Wayment B, Sheng X, Rodnick KJ, Centini R, Chen D, Litwin SE, Weimer BE, Abel ED.** Contribution of impaired myocardial insulin signaling to mitochondrial dysfunction and oxidative stress in the heart. *Circulation* 119: 1272–1283, 2009.
7. **Chaudhuri A, Ghanim H, Vora M, Sia CL, Korzeniewski K, Dhindsa S, Makdissi A, Dandona P.** Exenatide exerts a potent antiinflammatory effect. *J Clin Endocrinol Metab* 97: 198–207, 2012.
8. **Goto K, Iso T, Hanaoka H, Yamaguchi A, Suga T, Hattori A, Irie Y, Shinagawa Y, Matsui H, Syamsunarno MR, Matsui M, Haque A, Arai M, Kunimoto F, Yokoyama T, Endo K, Gonzalez FJ, Kurabayashi M.** Peroxisome proliferator-activated receptor-gamma in capillary endothelia promotes fatty acid uptake by heart during long-term fasting. *J Am Heart Assoc* 2: e004861, 2013.
9. **Gu HF, Ma J, Gu KT, Brismar K.** Association of intercellular adhesion molecule 1 (ICAM1) with diabetes and diabetic nephropathy. *Front Endocrinol (Lausanne)* 3: 179, 2012.
10. **Holst JJ, Gromada J.** Role of incretin hormones in the regulation of insulin secretion in diabetic and nondiabetic humans. *Am J Physiol Endocrinol Metab* 287: E199–E206, 2004.

11. **Hu E, Tontonoz P, Spiegelman BM.** Transdifferentiation of myoblasts by the adipogenic transcription factors PPAR gamma and C/EBP alpha. *Proc Natl Acad Sci USA* 92: 9856–9860, 1995.
12. **Huang C, Andres AM, Ratliff EP, Hernandez G, Lee P, Gottlieb RA.** Preconditioning involves selective mitophagy mediated by Parkin and p62/SQSTM1. *PLoS One* 6: e20975, 2011.
13. **Kim F, Pham M, Luttrell I, Bannerman DD, Tupper J, Thaler J, Hawn TR, Raines EW, Schwartz MW.** Toll-like receptor-4 mediates vascular inflammation and insulin resistance in diet-induced obesity. *Circ Res* 100: 1589–1596, 2007.
14. **Kondo K, Nozawa K, Tomita T, Ezaki K.** Inbred strains resulting from Japanese mice. *Bull Exp Anim* 6: 107–112, 1957.
15. **Lee YS, Park MS, Choung JS, Kim SS, Oh HH, Choi CS, Ha SY, Kang Y, Kim Y, Jun HS.** Glucagon-like peptide-1 inhibits adipose tissue macrophage infiltration and inflammation in an obese mouse model of diabetes. *Diabetologia* 55: 2456–2468, 2012.
16. **Maejima Y, Kuroda J, Matsushima S, Ago T, Sadoshima J.** Regulation of myocardial growth and death by NADPH oxidase. *J Mol Cell Cardiol* 50: 408–416, 2011.
17. **Mahadev K, Motoshima H, Wu X, Ruddy JM, Arnold RS, Cheng G, Lambeth JD, Goldstein BJ.** The NAD(P)H oxidase homolog Nox4 modulates insulin-stimulated generation of H_2O_2 and plays an integral role in insulin signal transduction. *Mol Cell Biol* 24: 1844–1854, 2004.
18. **Matsushima S, Kuroda J, Ago T, Zhai P, Park JY, Xie LH, Tian B, Sadoshima J.** Increased oxidative stress in the nucleus caused by Nox4 mediates oxidation of HDAC4 and cardiac hypertrophy. *Circ Res* 112: 651–663, 2013.
19. **Mells JE, Fu PP, Sharma S, Olson D, Cheng L, Handy JA, Saxena NK, Sorescu D, Anania FA.** Glp-1 analog, liraglutide, ameliorates hepatic steatosis and cardiac hypertrophy in C57BL/6J mice fed a Western diet. *Am J Physiol Gastrointest Liver Physiol* 302: G225–G235, 2012.
20. **Mundil D, Cameron-Vendrig A, Husain M.** GLP-1 receptor agonists: a clinical perspective on cardiovascular effects. *Diab Vasc Dis Res* 9: 95–108, 2012.
21. **Naik E, Dixit VM.** Mitochondrial reactive oxygen species drive proinflammatory cytokine production. *J Exp Med* 208: 417–420, 2011.
22. **Nikolaidis LA, Elahi D, Hentosz T, Doverspike A, Huerbin R, Zourelias L, Stolarski C, Shen YT, Shannon RP.** Recombinant glucagon-like peptide-1 increases myocardial glucose uptake and improves left ventricular performance in conscious dogs with pacing-induced dilated cardiomyopathy. *Circulation* 110: 955–961, 2004.
23. **Noyan-Ashraf MH, Momen MA, Ban K, Sadi AM, Zhou YQ, Riazi AM, Baggio LL, Henkelman RM, Husain M, Drucker DJ.** GLP-1R agonist liraglutide activates cytoprotective pathways and improves outcomes after experimental myocardial infarction in mice. *Diabetes* 58: 975–983, 2009.
24. **Noyan-Ashraf MH, Shikatani EA, Schuiki I, Mukovozov I, Wu J, Li RK, Volchuk A, Robinson LA, Billia F, Drucker DJ, Husain M.** A glucagon-like peptide-1 analog reverses the molecular pathology and cardiac dysfunction of a mouse model of obesity. *Circulation* 127: 74–85, 2013.
25. **Papanicolaou KN, Ngoh GA, Dabkowski ER, O'Connell KA, Ribeiro RF Jr, Stanley WC, Walsh K.** Cardiomyocyte deletion of mitofusin-1 leads to mitochondrial fragmentation and improves tolerance to ROS-induced mitochondrial dysfunction and cell death. *Am J Physiol Heart Circ Physiol* 302: H167–H179, 2012.
26. **Parlevliet ET, Wang Y, Geerling JJ, Schroder-Van der Elst JP, Picha K, O'Neil K, Stojanovic-Susulic V, Ort T, Havekes LM, Romijn JA, Pijl H, Rensen PC.** GLP-1 receptor activation inhibits VLDL production and reverses hepatic steatosis by decreasing hepatic lipogenesis in high-fat-fed APOE*3-leiden mice. *PLoS One* 7: e49152, 2012.
27. **Pattillo CB, Pardue S, Shen X, Fang K, Langston W, Jourd'heuil D, Kavanagh TJ, Patel RP, Kevil CG.** ICAM-1 cytoplasmic tail regulates endothelial glutathione synthesis through a NOX4/PI3-kinase-dependent pathway. *Free Radic Biol Med* 49: 1119–1128, 2010.
28. **Raddatz E, Thomas AC, Sarre A, Benathan M.** Differential contribution of mitochondria, NADPH oxidases, and glycolysis to region-specific oxidant stress in the anoxic-reoxygenated embryonic heart. *Am J Physiol Heart Circ Physiol* 300: H820–H835, 2011.
29. **Rijzewijk LJ, van der Meer RW, Smit JW, Diamant M, Bax JJ, Hammer S, Romijn JA, de Roos A, Lamb HJ.** Myocardial steatosis is an independent predictor of diastolic dysfunction in type 2 diabetes mellitus. *J Am Coll Cardiol* 52: 1793–1799, 2008.
30. **Roth P, Stanley ER.** The biology of CSF-1 and its receptor. *Curr Top Microbiol Immunol* 181: 141–167, 1992.
31. **Schaffer JE.** Lipotoxicity: when tissues overeat. *Curr Opin Lipidol* 14: 281–287, 2003.
32. **Schenk S, Saberi M, Olefsky JM.** Insulin sensitivity: modulation by nutrients and inflammation. *J Clin Invest* 118: 2992–3002, 2008.
33. **Shigeta T, Aoyama M, Bando YK, Monji A, Mitsui T, Takatsu M, Cheng XW, Okumura T, Hirashiki A, Nagata K, Murohara T.** Dipeptidyl peptidase-4 modulates left ventricular dysfunction in chronic heart failure via angiogenesis-dependent and -independent actions. *Circulation* 126: 1838–1851, 2012.
34. **Svegliati-Baroni G, Saccomanno S, Rychlicki C, Agostinelli L, De Minicis S, Candelaresi C, Faraci G, Pacetti D, Vivarelli M, Nicolini D, Garelli P, Casini A, Manco M, Mingrone G, Risaliti A, Frega GN, Benedetti A, Gastaldelli A.** Glucagon-like peptide-1 receptor activation stimulates hepatic lipid oxidation and restores hepatic signalling alteration induced by a high-fat diet in nonalcoholic steatohepatitis. *Liver Int* 31: 1285–1297, 2011.
35. **Taketomi S, Ikeda H, Ishikawa E, Iwatsuka H.** Determination of overall insulin sensitivity in diabetic mice, KK. *Horm Metab Res* 14: 14–18, 1982.
36. **van de Weijer T, Schrauwen-Hinderling VB, Schrauwen P.** Lipotoxicity in type 2 diabetic cardiomyopathy. *Cardiovasc Res* 92: 10–18, 2011.
37. **Wang Y, Nartiss Y, Steipe B, McQuibban GA, Kim PK.** ROS-induced mitochondrial depolarization initiates PARK2/PARKIN-dependent mitochondrial degradation by autophagy. *Autophagy* 8: 1462–1476, 2012.
38. **Yano T, Miura T, Whittaker P, Miki T, Sakamoto J, Nakamura Y, Ichikawa Y, Ikeda Y, Kobayashi H, Ohori K, Shimamoto K.** Macrophage colony-stimulating factor treatment after myocardial infarction attenuates left ventricular dysfunction by accelerating infarct repair. *J Am Coll Cardiol* 47: 626–634, 2006.
39. **Yoon YS, Uchida S, Masuo O, Cejna M, Park JS, Gwon HC, Kirchmair R, Bahlman F, Walter D, Curry C, Hanley A, Isner JM, Losordo DW.** Progressive attenuation of myocardial vascular endothelial growth factor expression is a seminal event in diabetic cardiomyopathy: restoration of microvascular homeostasis and recovery of cardiac function in diabetic cardiomyopathy after replenishment of local vascular endothelial growth factor. *Circulation* 111: 2073–2085, 2005.
40. **Zeyda M, Stulnig TM.** Obesity, inflammation, and insulin resistance—a mini-review. *Gerontology* 55: 379–386, 2009.

JACC: Heart Failure
© 2013 by the American College of Cardiology Foundation
Published by Elsevier Inc.

Vol. 1, No. 6, 2013
ISSN 2213-1779/$36.00
http://dx.doi.org/10.1016/j.jchf.2013.08.007

MINI FOCUS ISSUE: TRANSLATIONAL RESEARCH

Sarcomere Gene Mutations Are Associated With Increased Cardiovascular Events in Left Ventricular Hypertrophy

Results From Multicenter Registration in Japan

Takashi Fujita, MD,* Noboru Fujino, MD,* Ryuichiro Anan, MD,† Chuwa Tei, MD,† Toru Kubo, MD,‡ Yoshinori Doi, MD,‡ Shintaro Kinugawa, MD,§ Hiroyuki Tsutsui, MD,§ Shigeki Kobayashi, MD,|| Masafumi Yano, MD,|| Masanori Asakura, MD,¶ Masafumi Kitakaze, MD,¶ Issei Komuro, MD,# Tetsuo Konno, MD,* Kenshi Hayashi, MD,* Masa-aki Kawashiri, MD,* Hidekazu Ino, MD,* Masakazu Yamagishi, MD*

Kanazawa, Kagoshima, Nankoku, Sapporo, Ube, Suita, and Tokyo, Japan

Objectives This study investigated the occurrence of cardiovascular events in patients with hypertensive heart disease (HHD) or hypertrophic cardiomyopathy (HCM) with or without sarcomere gene mutations.

Background Although HHD and HCM are associated with left ventricular hypertrophy (LVH), few data exist regarding the difference in prognosis between them.

Methods We enrolled 256 patients with LVH (>13 mm) screened for sarcomere gene mutations. We divided them into 3 groups: the first had HHD without sarcomere gene mutations (group H), the second had sarcomere gene mutations (group G), and the third had neither sarcomere gene mutations nor HHD (group NG). We compared the occurrence of sudden cardiac death, ventricular tachycardia/fibrillation, admission for heart failure, and atrial fibrillation for 1 year.

Results Group G (n = 78, 36 men; mean age, 53.4 years) experienced more total cardiovascular events than group H (n = 45, 32 men; mean age, 67.4 years) (p = 0.042) after adjustments for age and sex, although there was no significant difference in total cardiovascular events between groups H and NG (n = 98, 66 men; mean age, 62.0 years). With Kaplan-Meier analysis, group G exhibited a significantly higher incidence of admission for heart failure (p = 0.017) and atrial fibrillation (p = 0.045) than group H in those 50 years of age and older. Additionally, there was a significant difference in total cardiovascular events between groups G and NG (p = 0.021).

Conclusions These results demonstrate that HCM with sarcomere gene mutations can be associated with increased cardiovascular events compared with HHD or HCM without sarcomere gene mutations. (J Am Coll Cardiol HF 2013;1:459–66) © 2013 by the American College of Cardiology Foundation

Left ventricular hypertrophy (LVH) is an independent predictor of the occurrence of cardiovascular events, even if left ventricular function is not impaired (1–3). The major causes of LVH include hypertrophic cardiomyopathy (HCM) and hypertensive heart disease (HHD) (4).

HCM is a primary myocardial disease, mainly caused by sarcomere gene mutations (5–9), that causes sudden cardiac death in the young or heart failure in the middle aged (3,10,11). Under these conditions, it is interesting to examine the differences in the prognosis of LVH between HCM and HHD. Therefore, in this multicenter, prospective trial, we investigated the difference in the occurrence of cardiovascular events between LVH patients with HCM with or without sarcomere gene mutations and with hypertension.

See page 467

From the *Division of Cardiovascular Medicine, Kanazawa University Graduate School of Medicine, Kanazawa, Japan; †Department of Cardiovascular, Respiratory and Metabolic Medicine, Kagoshima University, Kagoshima, Japan; ‡Department of Medicine and Geriatrics, Kochi Medical School, Nankoku, Japan; §Department of Cardiovascular Medicine, Hokkaido University School of Medicine, Sapporo, Japan; ||Department of Medicine and Clinical Science, Yamaguchi University Graduate School of Medicine, Ube, Japan; ¶Department of Clinical Research and Development, National Cerebral and Cardiovascular Center, Suita, Japan; and the #Department of Cardiovascular Medicine, University of Tokyo Graduate School of Medicine, Tokyo, Japan. This work was supported by a research grant for cardiovascular diseases (20C-4) from the Ministry of Health, Welfare, and Labor of Japan. The authors have reported that they have no relationships relevant to the contents of this paper to disclose. Part of this work was presented at the Annual Scientific Sessions, American Heart Association, 2012, Los Angeles, California.

Manuscript received December 13, 2012; revised manuscript received July 23, 2013, accepted August 9, 2013.

JACC: Heart Failure Vol. 1, No. 6, 2013
December 2013:459–66

Abbreviations and Acronyms

AF = atrial fibrillation
BNP = plasma B-type natriuretic peptide
BP = blood pressure
ECG = electrocardiographic
HCM = hypertrophic cardiomyopathy
HHD = hypertensive heart disease
ICD = implantable cardioverter-defibrillator
LVH = left ventricular hypertrophy
MR = mitral regurgitation
VF = ventricular fibrillation
VT = ventricular tachycardia

Methods

Study population. The Ethics Committee for Medical Research at our institutions approved the study protocol, and all patients provided written informed consent before participation. The study population comprised patients with suspected LVH by routine clinical examinations at 7 clinical institutions between September 2008 and March 2010. The follow-up survey was performed at the time of registration and after 1 year.

Clinical examinations. We performed echocardiography in all patients when the presence of LVH was suspected by routine clinical examinations. When LVH was confirmed by echocardiography, the patient was enrolled in this study. Plasma B-type natriuretic peptide (BNP) levels were also measured. The clinical diagnosis of HCM was based on the guidelines of the American College of Cardiology Foundation/European Society of Cardiology (12). The diagnosis of HHD was based on a history of long-term hypertension (systolic blood pressure [BP] ≥140 mm Hg and/or diastolic BP ≥90 mm Hg) and the absence of other cardiac or systemic diseases.

All of the patients continued appropriate medical treatment, such as beta-blockers, renin-angiotensin-aldosterone system inhibitors, calcium antagonists, and antiarrhythmic drugs. In addition, devices, such as a pacemaker and an implantable cardioverter-defibrillator, were also implanted if needed.

Echocardiographic examinations. Standard techniques were used for M-mode, 2-dimensional, and Doppler measurements. The severity and distribution of LVH were assessed by dividing the left ventricle into 5 regions: anterior, posterior, septal, and lateral segments in the parasternal short-axis view and the apical segment in the apical view. Wall thickness in the parasternal short-axis view was determined at the level of the mitral valve and the papillary muscles in each of the 4 segments. Maximal left ventricular wall thickness was defined as the greatest thickness within the chamber. The definition of LVH was based on a maximal left ventricular wall thickness >13 mm. Left ventricular outflow obstruction at rest was identified by a peak instantaneous left ventricular outflow tract pressure gradient ≥30 mm Hg. Other echocardiographic parameters were determined with methods recommended by the American Society of Echocardiography (13).

Genetic screening tests. Mutational analyses were performed using polymerase chain reaction and direct DNA sequencing for mutations in all translated exons of the 9 most common sarcomeric HCM genes: MYBPC3-encoded myosin binding protein C (*MYBPC3*), MYH7-encoded myosin heavy chain (*MYH7*), MYL2- and MYL3-encoded regulatory and essential myosin light chains (*MYL2* and *MYL3*, respectively), TNNI3-encoded troponin I (*TNNI3*), TNNT2-encoded cardiac troponin T (*TNNT2*), TPM1-encoded-tropomyosin (*TPM1*), TTN-encoded titin (*TTN*), and ACTC-encoded cardiac actin (*ACTC1*).

Evaluation of cardiovascular events. We investigated cardiovascular events such as sudden cardiac death,

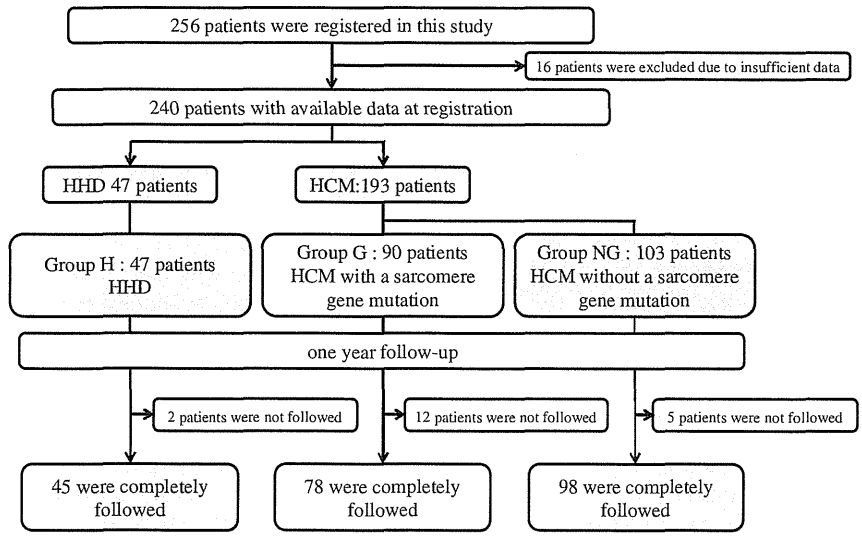

Figure 1 Study Enrollment and Flow of Patients

HCM = hypertrophic cardiomyopathy; HHD = hypertensive heart disease.

Table 1 Clinical Characteristics, Echocardiographic Data, Disease-Causing Gene, and Medication at Registration of All Patients

Variable	All Patients (N = 221)	Group H (n = 45)	All HCM (n = 176)	Group G (n = 78)	Group NG (n = 98)
Clinical characteristics					
Age, yrs	60.1 ± 17.0	67.4 ± 13.4	58.2 ± 17.4*	53.4 ± 20.0†	62.0 ± 13.9‡§
Male	134 (60.6)	32 (71.1)	102 (58.0)	36 (46.2)†	66 (67.3)§
Blood pressure, mm Hg					
Systolic	122.7 ± 18.6	135.4 ± 18.7	119.4 ± 17.1*	114.8 ± 16.9†	123.0 ± 16.5‡§
Diastolic	71.2 ± 11.6	76.1 ± 13.5	70.0 ± 10.8*	68.6 ± 11.6†	71.0 ± 10.0
Mean	88.0 ± 13.6	94.8 ± 13.6	86.4 ± 11.2*	84.0 ± 11.9†	88.3 ± 10.3‡§
Hypertension	61 (27.6)	45 (100.0)	16 (9.0)*	6 (7.7)†	10 (10.2)‡
Chronic AF	34 (15.4)	4 (8.9)	30 (17.0)	8 (10.3)	22 (22.4)§
ICD	25 (11.3)	1 (2.2)	19 (10.8)	9 (11.5)	10 (10.2)
BNP, pg/ml	274.0 ± 356.5	161.9 ± 233.5	285.4 ± 340.8*	288.0 ± 428.3†	283.4 ± 259.6‡
Echocardiography					
LAD, mm	44.2 ± 7.7	45.1 ± 6.1	44.0 ± 8.0	43.0 ± 8.6	44.8 ± 7.5
IVST, mm	16.0 ± 5.0	15.1 ± 3.9	16.2 ± 5.3	16.2 ± 5.7	16.3 ± 4.9
PLVWT, mm	10.8 ± 1.9	11.3 ± 1.6	10.6 ± 1.9*	10.1 ± 1.7†	11.1 ± 2.0§
MLVWT, mm	17.6 ± 4.7	16.0 ± 3.8	18.0 ± 4.9*	17.2 ± 5.5	18.6 ± 4.3‡
LVEDD, mm	46.7 ± 6.4	48.2 ± 5.3	46.3 ± 6.6*	46.2 ± 7.0†	46.4 ± 6.4
LVESD, mm	29.3 ± 7.4	30.1 ± 5.0	29.0 ± 7.9	29.9 ± 8.6	28.3 ± 7.1‡
LVEF, %	65.7 ± 12.3	65.6 ± 9.8	65.7 ± 12.9	64.3 ± 13.9	66.8 ± 12.0
LVOTPG >30 mm Hg	18 (8.1)	0 (0)	18 (10.2)*	5 (6.4)	13 (13.3)‡
Presence of MR	169 (76.5)	25 (55.6)	144 (81.8)*	58 (74.4)†	86 (87.8)‡§
Disease-causing gene					
MYBPC3				34 (43.6)	
TNNI3				23 (29.5)	
MYH7				15 (19.2)	
TNNT2				6 (7.7)	
Medication at registration					
Beta-blocker	101 (45.7)	20 (44.4)	81 (46.0)	31 (39.7)	50 (51.0)
Calcium antagonist	68 (30.8)	25 (55.6)	43 (24.4)*	20 (25.6)†	23 (23.5)‡
RAAS inhibitor	91 (41.2)	27 (60.0)	64 (36.4)*	32 (41.0)	32 (32.7)‡
Diuretic	48 (21.7)	12 (26.7)	36 (20.5)	19 (24.4)	17 (17.3)
Alpha-blocker	2 (0.9)	2 (4.4)	0 (0)*	0 (0)	0 (0)
Vitamin K antagonist	50 (22.6)	10 (22.2)	40 (22.7)	11 (14.1)	29 (29.6)§
Amiodarone	17 (7.7)	0 (0)	17 (9.7)*	9 (11.5)†	8 (8.2)

Values are mean ± SD or n (%). *p < 0.05, HHD vs. all HCM. †p < 0.05, group H vs. group G. ‡p < 0.05, group H vs. group NG. §p < 0.05, group G vs. group NG.

AF = atrial fibrillation; BNP = plasma B-type natriuretic peptide; ICD = implantable cardioverter-defibrillator; IVST = interventricular septum thickness; LAD = left atrial dimension; LVEDD = left ventricular end-diastolic dimension; LVESD = left ventricular end-systolic dimension; LVEF = left ventricular ejection fraction; LVOTPG = left ventricular outflow tract pressure gradient; MR = mitral regurgitation; MLVWT = maximal left ventricular wall thickness; PLVWT = posterior left ventricular wall thickness; RAAS = renin-angiotensin-aldosterone system. Group G = hypertrophic cardiomyopathy with sarcomere gene mutations; Group H = hypertensive heart disease; Group NG = hypertrophic cardiomyopathy without sarcomere gene mutations.

ventricular tachycardia (VT)/ventricular fibrillation (VF), admission for heart failure, and atrial fibrillation (AF) in all of the patients through a direct interview and with electrocardiography performed in the outpatient clinic or a telephone interview.

Documentation of AF was based on electrocardiographic (ECG) recordings obtained during provisional or routine medical examinations. Documentation of VT or VF was based on the occurrence of sudden cardiac death, records of VT/VF from an automated external defibrillator, or the use of an implantable cardioverter-defibrillator on Holter or continuous ECG monitoring. Nonsustained VT was defined as a minimum of 3 consecutive ventricular beats with a rate of >120 beats/min. The definition of admission caused by heart failure was that hospitalization was needed because of subjective or objective symptoms of heart failure.

Statistical analysis. Data are presented as the mean ± SD for continuous variables. Variables between the 2 groups were compared using the Mann-Whitney *U* test. Categorical frequencies were compared using the Fisher exact test, where appropriate. Survival estimates were calculated using Cox proportional hazards regression analysis or the Kaplan-Meier method, and their relationship was determined using the log-rank test for trend. A p value <0.05 was considered statistically significant. Data were analyzed using SPSS Statistics version 19.0 (SPSS Inc., Chicago, Illinois).

JACC: Heart Failure Vol. 1, No. 6, 2013
December 2013:459–66

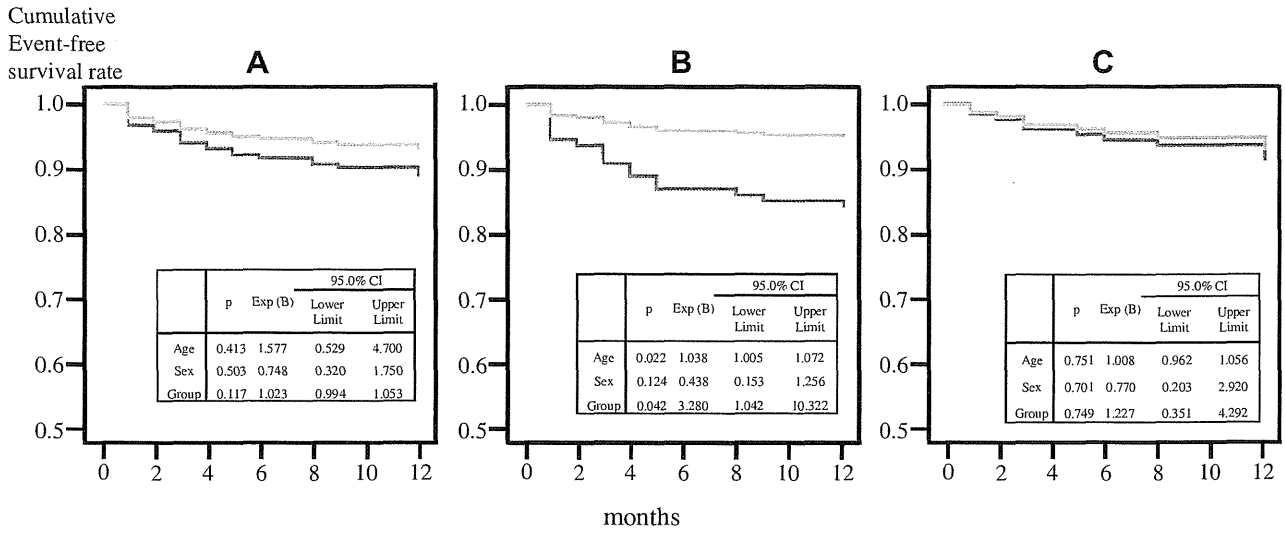

Figure 2 **Event-Free Survival in Total Cardiovascular Events With Cox Proportional Hazards Regression Analysis Adjusted for Age and Sex**

(A) All hypertrophic cardiomyopathy **(blue line)** and group H **(green line)**. **(B)** Groups G **(blue line)** and H **(green line)**. **(C)** Groups NG **(blue line)** and H **(green line)**. Group G = hypertrophic cardiomyopathy with sarcomere gene mutations; Group H = hypertensive heart disease; Group NG = hypertrophic cardiomyopathy without sarcomere gene mutations. CI = confidence interval.

Results

Over a period of 3 years, a total of 256 patients with LVH were enrolled. Sixteen patients were excluded because their data were insufficient at registration. Of the remaining 240 patients, 47 patients received a diagnosis of HHD and 193 patients HCM. Moreover, of the 193 patients with a diagnosis of HCM, 90 with a sarcomere gene mutation were registered in group G and 103 without a sarcomere gene mutation were registered in group NG (Fig. 1). Unfortunately, 2 patients in group H, 12 in group G, and 5 in group NG were excluded from the analysis because they changed their clinic after registration, interrupted their treatment, decided not to attend the follow-up of their own volition, or withdrew their consent. Therefore, no further information was obtained for these lost patients. Finally, a follow-up survey was completed in 45 patients in group H (32 men; mean age, 67.4 years), 78 in group G (36 men; mean age, 53.4 years), and 98 in group NG (66 men; mean age, 62.0 years) (Fig. 1).

First, we examined the difference in the prognosis of patients in group H and those with HCM (groups G and NG). The baseline characteristics of the 45 group H and 176 HCM patients are shown in Table 1. There were significant differences in age, BP, BNP levels, posterior wall thickness, maximal wall thickness, left ventricular end-diastolic dimension, left ventricular outflow tract pressure gradient, and presence of mitral regurgitation (MR) between both groups. It is important to note that, under these conditions, the imbalances of several potential confounders listed in Table 1 could mask differences between the groups as well as cause spurious associations. Even after adjusting for age and sex, there was no significant difference in total cardiovascular events between both groups with Cox proportional hazards regression analysis (hazard ratio: 1.023; 95% confidence interval: 0.994 to 1.053; p = 0.117) (Fig. 2A).

Next, we compared groups G and NG with group H. The baseline characteristics of groups G and NG are shown in Table 1. There were significant differences in age, sex, BP, BNP levels, posterior left ventricular wall thickness, left ventricular end-diastolic dimension, and the presence of MR between groups G and H, and significant differences in age, BP, BNP levels, maximal left ventricular wall thickness, left ventricular end-systolic dimension, left ventricular outflow tract pressure gradient, and presence of MR between groups NG and H. Six patients in group G and 10 in group NG also had high BP; however, these patients had no cardiovascular events, suggesting that this may have no impact on the present results. An ICD had been implanted in 1 patient in group H, 9 in group G, and 10 in group NG. Holter monitoring had been performed on 4 patients in group H, 23 in group G, and 30 in group NG. Under these conditions, for the identification of VT/VF, 6 patients were confirmed by Holter monitoring and 1 by checking their ICD, whereas 4 patients received shocks from an automated external defibrillator or ICD.

In group G, we identified 34 *MYBPC3* mutations, 23 *TNNI3* mutations, 15 *MYH7* mutations, and 6 *TNNT2* mutations (Table 1). The sarcomere gene mutation sites are

Table 2 Clinical Characteristics, Echocardiographic Data, Disease-Causing Gene, and Medication at Registration in Patients 50 Years of Age and Older in Groups G and H

Variable	All Patients (N = 86)	Group G (n = 45)	Group H (n = 41)
Clinical characteristics			
Age, yrs	69.0 ± 9.8	67.8 ± 10.5	70.5 ± 8.8
Male	53 (61.6)	24 (53.3)	29 (70.7)
Blood pressure, mm Hg			
Systolic	127.6 ± 19.4	120.3 ± 16.8	135.5 ± 19.0*
Diastolic	72.3 ± 12.2	70.0 ± 12.0	74.8 ± 12.2
Mean	90.7 ± 13.0	86.7 ± 11.9	95.0 ± 12.9*
Hypertension	46 (53.5)	5 (11.1)	41 (100.0)*
Chronic AF	11 (12.8)	7 (15.6)	4 (9.8)
ICD	6 (7.0)	5 (11.1)	1 (2.4)
BNP, pg/ml	213.8 ± 247.9	258.6 ± 251.5	171.3 ± 240.0*
Echocardiography			
LAD, mm	46.3 ± 6.5	47.6 ± 6.4	45.0 ± 6.3*
IVST, mm	15.5 ± 4.6	15.8 ± 5.2	15.1 ± 3.9
PLVWT, mm	10.9 ± 1.5	10.5 ± 1.4	11.2 ± 1.6*
MLVWT, mm	16.6 ± 4.3	17.1 ± 4.8	16.1 ± 3.8
LVEDD, mm	48.6 ± 6.3	49.2 ± 7.2	47.9 ± 5.2
LVESD, mm	31.8 ± 7.4	33.3 ± 9.0	30.2 ± 4.6
LVEF, %	62.3 ± 12.9	59.8 ± 15.1	65.1 ± 9.2
LVOTPG >30 mm Hg	3 (3.5)	3 (6.7)	0 (0)
Presence of MR	61 (70.9)	38 (84.4)	23 (56.1)*
Disease-causing gene			
MYBPC3		21 (46.7)	
TNNI3		11 (24.4)	
MYH7		9 (20.0)	
TNNT2		4 (8.9)	
Medication at registration			
Beta-blocker	37 (43.0)	19 (42.2)	18 (43.9)
Calcium antagonist	35 (40.7)	13 (28.9)	22 (53.7)*
RAAS inhibitor	52 (60.5)	28 (62.2)	24 (58.5)
Diuretic	28 (32.6)	17 (37.8)	11 (26.8)
Alpha-blocker	2 (2.3)	0 (0)	2 (4.9)
Vitamin K antagonist	19 (22.1)	9 (20.0)	10 (24.4)
Amiodarone	6 (7.0)	6 (13.3)	0 (0)*

*Values are mean ± SD or n (%). $p < 0.05$, group H vs. group G.
Abbreviations as in Table 1.

shown in Online Table 1. Most of these mutations have been identified and described elsewhere (7,9,14–19). Some novel mutations were presumed to be pathogenic by the standard criteria of the absence of the mutation in large numbers of normal controls, alteration of evolutionarily conserved residues, and/or predicted impact on protein structure. With respect to medication at registration, beta-blockers and renin-angiotensin-aldosterone system inhibitors were mainly used in these groups. Calcium antagonists were used more frequently in group H than in groups G and NG. Amiodarone was used in only 9 patients in group G and 8 in group NG.

Interestingly, Cox proportional hazards regression analysis, which was performed after adjusting for age and sex, demonstrated a significant difference in total cardiovascular events between groups H and G (hazard ratio: 3.28; 95% confidence interval: 1.042 to 10.322; $p = 0.042$) (Fig. 2B), although there was no significant difference in total cardiovascular events between groups H and NG (hazard ratio: 1.227; 95% confidence interval: 0.351 to 4.292; $p = 0.749$) (Fig. 2C).

With respect to groups H and G, when both groups were stratified in 10-year age groups and evaluated for the occurrence of cardiovascular events, few events were observed in patients younger than 50 years of age in both groups. Accordingly, both groups were re-evaluated for the occurrence of each cardiac event in a subgroup 50 years of age and older. There were 45 patients in group G and 41 in group H in this age group (Table 2). There were significant differences in BP, BNP levels, left atrial dimensions, posterior left ventricular wall thickness, and presence of MR between both groups in this age range. The sarcomere gene mutations sites of these patients in group G are shown in Online Table 2. Under these conditions, group G had significantly more admissions for heart failure ($p = 0.017$) and more AF ($p = 0.045$) than group H, although there was

JACC: Heart Failure Vol. 1, No. 6, 2013
December 2013:459–66

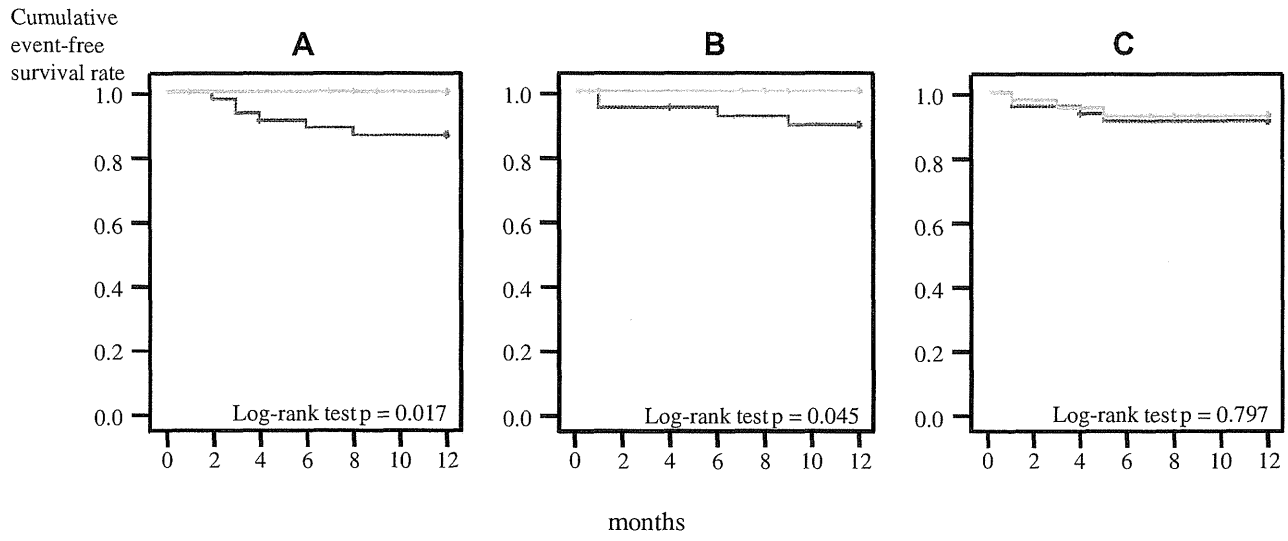

Figure 3 **Kaplan-Meier Analyses for Each Cardiovascular Event in Groups G and H in Patients 50 Years of Age and Older**

Group G = **blue line**; Group H = **green line**. **(A)** Rate of admission for heart failure. **(B)** Rate of atrial fibrillation. **(C)** Rate of ventricular tachycardia/ventricular fibrillation. Abbreviations as in Figure 2.

no significant difference in VT/VF (p = 0.797) between both groups (Fig. 3).

It is interesting to examine the relationship between disease-causing mutations and cardiovascular events. There were mutations in *TNNI3* in 2 patients, in *MYBPC3* in 2, in *TNNT2* in 1, and in *MYH7* in 1 of those admitted for heart failure, and there were mutations in *TNNI3* in 1 patient, in *MYBPC3* in 1, in *TNNT2* in 1, and in *MYH7* in 1 of those with AF. There was no significant relationship between the kind of disease-causing gene and the occurrence of cardiovascular events in this cohort. Additionally, when we divided group G according to the presence or absence of an *MYBPC3* mutation because of the high prevalence of *MYBPC3* in the present study, there was no significant difference in cardiovascular events between the subgroups.

It is intriguing to compare the occurrence of cardiovascular events between groups G and NG. Cox proportional hazards regression analysis, adjusting for age and sex, demonstrated a significant difference in total cardiovascular events between groups G and NG (hazard ratio: 3.031; 95% confidence interval: 1.183 to 7.764; p = 0.021) (Online Fig. 1). Also, there was a significant difference in AF (p = 0.036) between groups G and NG, although there was no significant difference in admission for heart failure (p = 0.172) and VT/VF (p = 0.288) between groups G and NG.

Discussion

The present study demonstrates that there are significantly more total cardiovascular events in 1 year in group G than in groups H and NG after adjusting for age and sex, although there was no significant difference in cardiovascular events between group H and group G with NG or between groups H and NG. This suggests that sarcomere gene mutations are associated with increased cardiovascular events in LVH, although HCM without sarcomere gene mutations did not increase the risk compared with HHD after 1 year. These results are consistent with previous reports in which HCM with a sarcomere gene mutation had an increased frequency of cardiovascular events over time (9,20–22).

In the subgroup 50 years of age and older, there was a higher occurrence of admission for heart failure and AF in group G than in group H. There was no admission for heart failure in group H, although BP was significantly higher in this group, even with the use of antihypertensive drugs. This suggests that if the target BP is achieved with antihypertensive treatment, the development of heart failure can be inhibited, thereby improving the survival rate of patients with HHD (1,23–25). Conversely, HCM with sarcomere gene mutation is a progressive disease; indeed, Ho et al. (26) demonstrated the early occurrence of myocardial fibrosis in HCM patients with sarcomere gene mutations. The initial medical therapy for HCM is negative inotropic agents, such as beta-blockers, verapamil, and disopyramide (12,27–29), as was also observed in the present study. However, these agents have not been shown to suppress or induce the regression of cardiac hypertrophy or myocardial fibrosis. Moreover, BNP levels were significantly higher in group G than in group H, although the left ventricular ejection fraction was not significantly

different between both groups. This suggests that left ventricular diastolic function was more highly impaired in group G than in group H. In groups G and NG, there were no significant differences in BNP levels and left ventricular ejection fraction. This may explain why there was no significant difference in admission for heart failure between groups G and NG in the present study.

It is important to note the impact of amiodarone on the occurrence of arrhythmias. With regard to AF, only 1 of 6 patients 50 years of age and older in group G taking amiodarone had AF. Therefore, amiodarone had little effect. The higher prevalence of MR and larger atrial dimensions in patients 50 years of age and older in group G than in group H might contribute to the higher occurrence of AF in group G, as described in a previous report (30).

Study limitations. First, the ratio of sarcomere gene mutations in this study was somewhat different from that generally reported, despite the multicenter nature of the present study (5,31). This mutation bias might affect the frequency of cardiovascular events. However, this bias could have little impact on the present results because there was no significant difference in the occurrence of cardiovascular events among the different sarcomere gene mutation carriers in the present cohort. Second, some cases of nonsustained VT could have been missed because Holter or continuous ECG monitoring was not performed in all patients. However, this disadvantage could be minimized by careful interview regarding the occurrence of arrhythmias. Third, there is no standard protocol for the use of therapeutic medicines, and each doctor's judgment was entrusted. However, they administered the therapeutic medications according to major guidelines (12,32,33). Actually, there was no major difference in the medications used among the participating facilities. Finally, LVH progresses slowly, and a long-term follow-up study is required. However, there was a significant difference in cardiovascular events even after a 1 year follow-up, suggesting the clinical significance of gene mutations in LVH patients.

Conclusions

The present study demonstrates that HCM with sarcomere gene mutations can be associated with increased cardiovascular events compared with HHD and HCM without sarcomere gene mutations. We suggest that the elucidation of the cause of LVH, particularly the identification of sarcomere gene mutations, is important for the determination of the prognosis in LVH patients.

Reprint requests and correspondence: Dr. Masakazu Yamagishi, Division of Cardiovascular Medicine, Kanazawa University Graduate School of Medicine, 13-1, Takara-machi, Kanazawa, Ishikawa 920-8641, Japan. E-mail: myamagi@med.kanazawa-u.ac.jp.

REFERENCES

1. Pierdomenico SD, Lapenna D, Cuccurullo F. Regression of echocardiographic left ventricular hypertrophy after 2 years of therapy reduces cardiovascular risk in patients with essential hypertension. Am J Hypertens 2008;21:464–70.
2. de Simone G, Verdecchia P, Pede S, Gorini M, Maggioni AP. Prognosis of inappropriate left ventricular mass in hypertension: the MAVI Study. Hypertension 2002;40:470–6.
3. Levy D, Garrison RJ, Savage DD, Kannel WB, Castelli WP. Prognostic implications of echocardiographically determined left ventricular mass in the Framingham Heart Study. N Engl J Med 1990;322:1561–6.
4. Misawa K, Nitta Y, Matsubara T, et al. Difference in coronary blood flow dynamics between patients with hypertension and those with hypertrophic cardiomyopathy. Hypertens Res 2002;25:711–6.
5. Marian AJ, Roberts R. The molecular genetic basis for hypertrophic cardiomyopathy. J Mol Cell Cardiol 2001;33:655–70.
6. Fujino N, Shimizu M, Ino H, et al. A novel mutation Lys273Glu in the cardiac troponin T gene shows high degree of penetrance and transition from hypertrophic to dilated cardiomyopathy. Am J Cardiol 2002;89:29–33.
7. Kokado H, Shimizu M, Yoshio H, et al. Clinical features of hypertrophic cardiomyopathy caused by a Lys183 deletion mutation in the cardiac troponin I gene. Circulation 2000;102:663–9.
8. Anan R, Shono H, Kisanuki A, Arima S, Nakao S, Tanaka H. Patients with familial hypertrophic cardiomyopathy caused by a Phe110Ile missense mutation in the cardiac troponin T gene have variable cardiac morphologies and a favorable prognosis. Circulation 1998;98:391–7.
9. Kubo T, Kitaoka H, Okawa M, et al. Lifelong left ventricular remodeling of hypertrophic cardiomyopathy caused by a founder frameshift deletion mutation in the cardiac Myosin-binding protein C gene among Japanese. J Am Coll Cardiol 2005;46:1737–43.
10. Maron BJ, Shirani J, Poliac LC, Mathenge R, Roberts WC, Mueller FO. Sudden death in young competitive athletes. Clinical, demographic, and pathological profiles. JAMA 1996;276:199–204.
11. Monserrat L, Elliott PM, Gimeno JR, Sharma S, Penas-Lado M, McKenna WJ. Non-sustained ventricular tachycardia in hypertrophic cardiomyopathy: an independent marker of sudden death risk in young patients. J Am Coll Cardiol 2003;42:873–9.
12. Maron BJ, McKenna WJ, Danielson GK, et al. American College of Cardiology/European Society of Cardiology clinical expert consensus document on hypertrophic cardiomyopathy. A report of the American College of Cardiology Foundation Task Force on Clinical Expert Consensus Documents and the European Society of Cardiology Committee for Practice Guidelines. J Am Coll Cardiol 2003;42:1687–713.
13. Lang RM, Bierig M, Devereux RB, et al. Recommendations for chamber quantification: a report from the American Society of Echocardiography's Guidelines and Standards Committee and the Chamber Quantification Writing Group, developed in conjunction with the European Association of Echocardiography, a branch of the European Society of Cardiology. J Am Soc Echocardiogr 2005;18:1440–63.
14. Van Driest SL, Jaeger MA, Ommen SR, et al. Comprehensive analysis of the beta-myosin heavy chain gene in 389 unrelated patients with hypertrophic cardiomyopathy. J Am Coll Cardiol 2004;44:602–10.
15. Watkins H, McKenna WJ, Thierfelder L, et al. Mutations in the genes for cardiac troponin T and alpha-tropomyosin in hypertrophic cardiomyopathy. N Engl J Med 1995;332:1058–64.
16. Anan R, Niimura H, Takenaka T, Hamasaki S, Tei C. Mutations in the genes for sarcomeric proteins in Japanese patients with onset sporadic hypertrophic cardiomyopathy after age 40 years. Am J Cardiol 2007;99:1750–4.
17. Anan R, Niimura H, Minagoe S, Tei C. A novel deletion mutation in the cardiac myosin-binding protein C gene as a cause of Maron's type IV hypertrophic cardiomyopathy. Am J Cardiol 2002;89:487–8.
18. Hirota T, Kubo T, Kitaoka H, et al. A novel cardiac myosin-binding protein C S297X mutation in hypertrophic cardiomyopathy. J Cardiol 2010;56:59–65.
19. Fujino N, Konno T, Hayashi K, et al. Impact of systolic dysfunction in genotyped hypertrophic cardiomyopathy. Clin Cardiol 2013;36:160–5.

JACC: Heart Failure Vol. 1, No. 6, 2013
December 2013:459–66

20. Moolman JC, Corfield VA, Posen B, et al. Sudden death due to troponin T mutations. J Am Coll Cardiol 1997;29:549–55.
21. Ashrafian H, Watkins H. Reviews of translational medicine and genomics in cardiovascular disease: new disease taxonomy and therapeutic implications cardiomyopathies: therapeutics based on molecular phenotype. J Am Coll Cardiol 2007;49:1251–64.
22. Olivotto I, Girolami F, Ackerman MJ, et al. Myofilament protein gene mutation screening and outcome of patients with hypertrophic cardiomyopathy. Mayo Clin Proc 2008;83:630–8.
23. Klingbeil AU, Schneider M, Martus P, Messerli FH, Schmieder RE. A meta-analysis of the effects of treatment on left ventricular mass in essential hypertension. Am J Med 2003;115:41–6.
24. Pitt B, Reichek N, Willenbrock R, et al. Effects of eplerenone, enalapril, and eplerenone/enalapril in patients with essential hypertension and left ventricular hypertrophy: the 4E-left ventricular hypertrophy study. Circulation 2003;108:1831–8.
25. Okin PM, Devereux RB, Jern S, et al. Regression of electrocardiographic left ventricular hypertrophy during antihypertensive treatment and the prediction of major cardiovascular events. JAMA 2004;292:2343–9.
26. Ho CY, López B, Coelho-Filho OR, et al. Myocardial fibrosis as an early manifestation of hypertrophic cardiomyopathy. N Engl J Med 2010;363:552–63.
27. Spirito P, Seidman CE, McKenna WJ, Maron BJ. The management of hypertrophic cardiomyopathy. N Engl J Med 1997;336:775–85.
28. Wigle ED, Rakowski H, Kimball BP, Williams WG. Hypertrophic cardiomyopathy. Clinical spectrum and treatment. Circulation 1995; 92:1680–92.
29. Maron BJ. Hypertrophic cardiomyopathy: a systematic review. JAMA 2002;287:1308–20.
30. Psaty BM, Manolio TA, Kuller LH, et al. Incidence of and risk factors for atrial fibrillation in older adults. Circulation 1997;96:2455–61.
31. Morita H, Larson MG, Barr SC, et al. Single-gene mutations and increased left ventricular wall thickness in the community: the Framingham Heart Study. Circulation 2006;113:2697–705.
32. Gersh BJ, Maron BJ, Bonow RO, et al. 2011 ACCF/AHA guideline for the diagnosis and treatment of hypertrophic cardiomyopathy: a report of the American College of Cardiology Foundation/American Heart Association Task Force on Practice Guidelines. Developed in collaboration with the American Association for Thoracic Surgery, American Society of Echocardiography, American Society of Nuclear Cardiology, Heart Failure Society of America, Heart Rhythm Society, Society for Cardiovascular Angiography and Interventions, and Society of Thoracic Surgeons. J Am Coll Cardiol 2011; 58:e212–60.
33. Ogihara T, Kikuchi K, Matsuoka H, et al. The Japanese Society of Hypertension Guidelines for the Management of Hypertension (JSH 2009). Hypertens Res 2009;32:3–107.

Key Words: heart failure ▪ left ventricular hypertrophy ▪ prognosis ▪ sarcomere gene mutations.

APPENDIX

For supplemental tables and figure, please see the online version of this article.

Persistent Overexpression of Phosphoglycerate Mutase, a Glycolytic Enzyme, Modifies Energy Metabolism and Reduces Stress Resistance of Heart in Mice

Junji Okuda[1☯], Shinnichiro Niizuma[1☯], Tetsuo Shioi[1]*, Takao Kato[1], Yasutaka Inuzuka[1], Tsuneaki Kawashima[1], Yodo Tamaki[1], Akira Kawamoto[1], Yohei Tanada[1], Yoshitaka Iwanaga[1], Michiko Narazaki[2], Tetsuya Matsuda[2], Souichi Adachi[3], Tomoyoshi Soga[4], Genzou Takemura[5], Hiroshi Kondoh[6], Toru Kita[1], Takeshi Kimura[1]

1 Department of Cardiovascular Medicine, Graduate School of Medicine, Kyoto University, Kyoto, Japan, **2** Department of Systems Science, Graduate School of Informatics, Kyoto University, Kyoto, Japan, **3** Human Health Sciences, Graduate School of Medicine, Kyoto University, Kyoto, Japan, **4** Institute for Advanced Biosciences, Keio University, Tsuruoka, Japan, **5** Division of Cardiology, Gifu University Graduate School of Medicine, Gifu, Japan, **6** Department of Geriatric Medicine, Graduate School of Medicine, Kyoto University, Kyoto, Japan

Abstract

Background: Heart failure is associated with changes in cardiac energy metabolism. Glucose metabolism in particular is thought to be important in the pathogenesis of heart failure. We examined the effects of persistent overexpression of phosphoglycerate mutase 2 (Pgam2), a glycolytic enzyme, on cardiac energy metabolism and function.

Methods and Results: Transgenic mice constitutively overexpressing Pgam2 in a heart-specific manner were generated, and cardiac energy metabolism and function were analyzed. Cardiac function at rest was normal. The uptake of analogs of glucose or fatty acids and the phosphocreatine/βATP ratio at rest were normal. A comprehensive metabolomic analysis revealed an increase in the levels of a few metabolites immediately upstream and downstream of Pgam2 in the glycolytic pathway, whereas the levels of metabolites in the initial few steps of glycolysis and lactate remained unchanged. The levels of metabolites in the tricarboxylic acid (TCA) cycle were altered. The capacity for respiration by isolated mitochondria *in vitro* was decreased, and that for the generation of reactive oxygen species (ROS) *in vitro* was increased. Impaired cardiac function was observed in response to dobutamine. Mice developed systolic dysfunction upon pressure overload.

Conclusions: Constitutive overexpression of Pgam2 modified energy metabolism and reduced stress resistance of heart in mice.

Citation: Okuda J, Niizuma S, Shioi T, Kato T, Inuzuka Y, et al. (2013) Persistent Overexpression of Phosphoglycerate Mutase, a Glycolytic Enzyme, Modifies Energy Metabolism and Reduces Stress Resistance of Heart in Mice. PLoS ONE 8(8): e72173. doi:10.1371/journal.pone.0072173

Editor: Junichi Sadoshima, Rutgers New Jersey Medical School, United States of America

Received December 19, 2012; **Accepted** July 10, 2013; **Published** August 12, 2013

Funding: This work was supported by the Japan Society for the Promotion of Science, the Vehicle Racing Commemorative Foundation, and the Innovative Techno-Hub for Integrated Medical Bio-imaging Project of the Special Coordination Funds for Promoting Science and Technology. The funders had no role in study design, data collection and analysis, decision to publish, or preparation of the manuscript.

Competing Interests: The authors have declared that no competing interests exist.

* E-mail: tshioi@kuhp.kyoto-u.ac.jp

☯ These authors contributed equally to this work.

Introduction

Heart failure is becoming a serious health care problem. It is a typical age-related disease, and the number of patients with heart failure continues to increase [1]. Moreover, it is the most frequent cause of rehospitalization in all cases of disease [2]. However, even with the best treatment, the annual rate of mortality from heart failure is still as high as 10%. Thus, the development of new treatments is a major challenge in cardiology [1]. The development and progression of heart failure is associated with changes in cardiac energy metabolism, including altered substrate utilization, abnormal mitochondrial function, and a decrease in energy transfer due to creatine shuttle dysfunction [3]. Among these changes, modulating substrate utilization appears to be a promising therapeutic target. Partial inhibition of fatty acid utilization, which is likely to increase glucose metabolism, has been shown to ameliorate cardiac dysfunction in patients with heart failure [4]. A previous study showed that a β-adrenergic receptor blocker shifted substrate utilization from fatty acids to glucose [5].

How substrate utilization is altered in patients with heart failure remains controversial. Previous studies reported that fatty acid utilization in patients with heart failure was increased [6,7] or decreased [8]. Glucose utilization in patients with heart failure has been reported to increase [8,9] as well as decrease [6,7]. Fatty acid utilization was shown to be unchanged [10] or decreased [11] in animal models of heart failure, while glucose utilization increased in animals with cardiac hypertrophy [12] or heart failure [11]. We reported previously that the uptake of an analog of fatty acids was

decreased and that of glucose was increased in a rat model of heart failure [13].

Cardiac-specific overexpression of glucose transporter 1 (GLUT1) was shown to result in increased glucose uptake, glycolysis, and decreased fatty acid oxidation, and also prevents systolic dysfunction and left ventricular dilatation in mice subjected to pressure overload induced by ascending aortic constriction [14]. Pyruvate dehydrogenase kinase (PDK) inactivates pyruvate dehydrogenase, the rate-limiting enzyme of glycolysis. Cardiac-specific overexpression of pyruvate dehydrogenase kinase 4 (PDK4) in transgenic mice has been shown to decrease glucose oxidation and increase fatty acid catabolism, and predispose animals to heart failure [15]. The potential advantage to increasing glucose utilization is that utilizing glucose as an energy source stoichiometrically requires less oxygen than that of fatty acids to produce the same amount of adenosine triphosphate (ATP) [16].

The phosphoglycerate mutase (Pgam) protein is an important enzyme in the glycolytic pathway and catalyzes the transfer of phosphate groups from 3-phosphoglycerate to 2-phosphoglycerate. This enzyme functions as a dimer and has been highly conserved throughout evolution. Mammals express two isoforms, one of which is brain-specific (Pgam1) while the other is muscle-specific (Pgam2) [17]. The overexpression of Pgam2 using a retroviral vector in primary mouse embryonic fibroblasts (MEFs) was shown to enhance glycolysis [18]. In humans, a deficiency in phosphoglycerate mutase caused glycogen storage disease type X, characterized by exercise intolerance and cramps [19]. Tissue Pgam1 protein levels were increased and associated with poor clinical outcome in patients with lung cancer [20]. Moreover, inhibiting the Pgam1 protein was shown to attenuate tumor growth [21]. A small-molecule inhibitor of the Pgam1 protein has been developed [22].

Heart tissue has the second highest level of Pgam activity, next to skeletal muscle [23]. Pgam2 protein expression increased approximately 5-fold in a canine model of tachycardia-induced heart failure [24]. These results indicate that Pgam2 may be involved in the development of heart failure. To examine the role of Pgam2 in the heart, we generated transgenic mice constitutively overexpressing Pgam2 in a heart-specific manner and analyzed cardiac energy metabolism and function.

Materials and Methods

1. Animals.

Transgenic lines overexpressing murine Pgam2 in a heart-specific manner were generated on a C57BL/6J (C57BL6) background using the murine α-myosin heavy chain (α-MHC) promoter [25], and were designated Pgam2 mice. The expression of the α-MHC promoter markedly increases several days after birth and remains high throughout the lifetime of these mice [26]. Transgenic mice and non-transgenic (NTg) littermates as controls were maintained on a 12-h light/dark cycle, fed a normal laboratory diet *ad libitum*, sacrificed by decapitation under ether anesthesia at 3 months of age, and analyzed. Hearts were resected immediately, washed in cold phosphate-buffered saline (PBS), divided into 3 parts, snap-frozen in liquid nitrogen, and stored at -80°C. Ventricular tissues were used for western blotting, enzymatic activity assays, metabolomic analysis, measuring mitochondrial oxygen consumption and hydrogen peroxide (H_2O_2) generation, and histological analysis. This investigation conformed to the Guide for the Care and Use of Laboratory Animals published by the US National Institutes of Health (NIH Publication No. 85-23, revised 1996). All animal care, experiments, and methods were approved by the Animal Care and Use Committees of Kyoto University Graduate School of Medicine.

2. Western blotting.

Total protein was extracted from frozen hearts, resolved, electrophoresed, and electrotransferred to a nitrocellulose membrane as described previously [27]. The antibodies used for western blotting were those against Pgam1 (1:1000, Abcam, Cambridge, UK; Ab2220), Myc (9E10) (1:1000; Santa Cruz Biotechnology, Santa Cruz, CA, USA; sc-40), and glyceraldehyde 3-phosphate dehydrogenase (GAPDH) (1:2000; Chemicon International, Temecula, CA, USA; 6C5).

3. Measuring Pgam and phosphofructokinase (PFK) activity.

The assay of phosphoglycerate mutase activity, measured via activity-based nicotinamide adenine dinucleotide (NADH)-consuming spectrophotometry, was performed as described [18]. Fifteen μg of tissue lysate was incubated with NADH (0.2 mmol/L; Sigma, St. Louis, MO, USA; N7410), adenosine diphosphate (ADP) (1.5 mmol/L, Sigma, A4386), 2,3-diphosphoglycerate (10 μmol/L, Sigma, D9134), lactate dehydrogenase (200 milliunits, Sigma, L1254), pyruvate kinase (170 milliunits, Sigma, P7768), and enolase (35 milliunits, Sigma, E0379) at 37°C for 10 minutes for the Pgam assay. The reaction was started by adding 3-phosphoglyceric acid (3-PGA) (1 mmol/L final concentration, Sigma, P8877) as a substrate to the assay mixture. The reduced form (NADH) and not the oxidized form (NAD^+) absorbs ultraviolet rays at 340 nm, and absorbance at 340 nm was previously shown to be proportional to the concentration of NADH; therefore, we monitored the decrease in absorbance of the above reaction mixture at 340 nm under incubation at 37°C over a time period of 12 minutes in a Spectra max M2^e plate reader (Molecular Devices, Menlo Park, CA, USA). Phosphofructokinase (PFK) activity was measured using the Phosphofructokinase Activity Colorimetric Assay Kit (BioVision, Milpitas, CA, USA; K776-100), according to the manufacturer's instructions. Briefly, PFK converts fructose-6-phosphate (F6P) and ATP to fructose-diphosphate and ADP. ADP is then converted to adenosine monophosphate (AMP) and NADH in the presence of the substrate and enzyme mix. NADH reduces a colorless probe to a colored product that exhibits strong absorbance at 450 nm. We measured absorbance at 450 nm to analyze the amount of NADH produced, which reflected PFK activity levels.

4. Cardiac echocardiography.

Cardiac echocardiography was performed as described previously, using an intraperitoneal injection of 2-2-2 tribromoethanol (240 mg/kg, Wako Pure Chemical, Kyoto, Japan) as an anesthetic [27,28].

5. Myocardial uptake of glucose and fatty acids.

Myocardial uptake of glucose and fatty acids was analyzed using the analogs ^{18}F-fluorodeoxyglucose (^{18}FDG) and ^{125}I-labeled 15-(*p*-iodophenyl)-9-*R*,*S*-methylpentadecanoic acid (^{125}I-9MPA), respectively, as previously described [13]. The amount of radioisotope incorporated was presented as a standard uptake value (SUV). SUV: tissue concentration (MBq/g)/(injected dose (MBq)/body weight (g)).

6. In situ ^{31}P magnetic resonance spectroscopy (MRS).

Myocardial energy reserve was measured by *in situ* ^{31}P magnetic resonance spectroscopy (MRS) using a Bruker Biospec 70/20 USR

system (Bruker Biospin, Ettlingen, Germany) with a 20-mm-diameter $^{1}H/^{31}P$ surface coil as described [29]. Isoflurane (2%) was used for anesthesia. The phosphocreatine (PCr)/βATP ratio was calculated by dividing PCr resonance by that of β-ATP and was used as an index of cardiac energy reserve.

7. Metabolomic Analysis of Pgam2 mice.

The ventricular heart tissue of Pgam2 mice and their NTg littermates at 3 months of age (n = 5 in each group) was subjected to metabolomic analysis as described [13]. Capillary electrophoresis time-of-flight mass spectrometry (CE-TOFMS) was used for metabolomic analysis [30]. We measured the levels of metabolites in glycolysis and the tricarboxylic acid (TCA) cycle, and amino acids and their derivatives.

8. Quantitative real-time polymerase chain reaction (PCR).

Preparing RNA and quantitative real-time PCR were performed as described previously [28]. The level of each mRNA was normalized with 18S ribosomal mRNA as an endogenous control. The genes and primer sequences analyzed are listed in Table S1.

9. Measurement of oxygen consumption using isolated mitochondria.

Mitochondria were isolated from the heart as described previously [31]. Mitochondria obtained by this method were likely to be in the subsarcolemmal fraction [31]. Oxygen consumption by isolated mitochondria was measured using a Clark oxygen electrode cuvette (Yellow Springs Instruments, Yellow Springs, OH, USA), as described [32]. Briefly, substrates and inhibitors corresponding to individual segments of the electron transport pathway were added in turn to samples in the oxygen electrodes in the following final concentrations (5 mM malate + 5 mM pyruvate, 100 nM rotenone, 5 mM succinate, 1 mM adenosine diphosphate, 50 nM antimycin A, 0.4 mM N,N,N',N'-tetramethyl-p-phenylenediamine (TMPD) + 1 mM ascorbate, and 5 mM potassium cyanide).

10. Measuring mitochondrial H_2O_2 generation using isolated mitochondria.

Mitochondria were isolated using a Qproteome Mitochondria Isolation Kit (Qiagen, Valencia, CA, USA), and mitochondrial H_2O_2 release was measured in the presence of horseradish peroxidase using an Amplex Red Hydrogen Peroxide/Peroxidase Assay kit (Molecular Probes, Carlsbad, CA, USA) as described [32]. The substrates used were 2.5 mM malate + 2.5 mM pyruvate or 5 mM succinate. Measurements were performed with 96-well plates under incubation at 37°C. Fluorometric measurements were performed with excitation at 544 nm and emission at 590 nm.

11. Transmission electron microscopy.

Cardiac tissue from the left ventricle was quickly cut into 1 mm cubes, immersion-fixed with 2.5% glutaraldehyde in 0.1 mol/L phosphate buffer (pH 7.4) overnight at 4°C, and fixed in 1% buffered osmium tetroxide. Specimens were subsequently dehydrated through a graded ethanol series and embedded in epoxy resin. Ultrathin slices (90 nm) were double-stained with uranyl acetate and lead citrate, and observed under an electron microscope (H-800, Hitachi, Tokyo, Japan). Morphometrical analyses were performed as described [33].

12. Measuring thiobarbituric acid reactive substrates (TBARS).

TBARS levels in left ventricular tissue were measured according to the manufacturer's instructions (Alexis Biochemicals, Lausen, Switzerland).

13. Cardiac hemodynamics in vivo assessed by cardiac catheterization under dobutamine infusion.

Left ventricular functional reserve was analyzed by cardiac catheterization under dobutamine infusion as reported previously. Isoflurane (2%) was used for anesthesia [28]. LV pressure signals of 10 to 20 beats were averaged and analyzed with PowerLab software (Chart 5, AD Instruments, Dunedin, New Zealand).

14. Surgical procedures for transverse aortic constriction (TAC).

Transverse aortic constriction (TAC) or a sham operation was performed on 12-week-old male NTg and Pgam2 mice as described previously [34]. Briefly, a 7-0 silk string ligature was tied around a 26-gauge needle and the needle was then removed to constrict the transverse aorta. Mice were sacrificed and analyzed 14 days after aortic constriction.

15. Measuring myocardial fibrosis.

Hearts were fixed in 4% paraformaldehyde (PFA), embedded in paraffin, and sectioned (10 μm) for histological evaluation. Sirius Red staining was performed and images were captured and digitized using an image analyzing light microscopy system (KEYENCE BioZero BZ-8000). To quantify the area of myocardial interstitial fibrosis, the red pixel content of the digitized photos was measured relative to the total tissue area using Adobe Photoshop 7.0.1 software (Adobe Systems, San Jose, CA, USA).

16. Statistical analysis.

Values are expressed as the mean ± SEM for each experimental group. ANOVA was used for comparisons between multiple groups. The Student's *t* test was used for comparisons between 2 groups. In all tests, a value of $p<0.05$ was considered significant.

Results

1. Generation of transgenic mice constitutively overexpressing Pgam2 in the heart.

Transgenic mice overexpressing murine Pgam2 in a heart-specific manner were generated using the α-MHC promoter on a C57BL6 background. Five independently derived founders were produced from 43 screened mice. The progenies of 4 of the 5 founders expressed the transgene product as determined by PCR. The progeny of 3 of the 4 founders expressed the transgene product as determined by western blot analysis. The Pgam1 antibody detected both mouse PGAM1 and PGAM2 at a similar sensitivity (Figure S1). Migration of the transgene product, the Pgam2 protein with a Myc-tag, was slower than that of the endogenous Pgam protein on a sodium dodecyl sulfate polyacrylamide gel electrophoresis (SDS-PAGE) gel (Figure 1A). Two of the 3 lines of Pgam2 mice (line 22 (L22) and line 38 (L38)) expressed different total Pgam protein levels in the heart (9.7-fold and 12.6-fold, in which measurements included endogenous Pgam relative to levels in non-transgenic (NTg) mice, respectively). To confirm the accentuation of phosphoglycerate mutase enzymatic activity in Pgam2-transgenic mice, the half-time of absorbance at 340 nm to the completion of the reaction, which represented the amount of NADH consumed, was calculated in Pgam2 (L38) mice. The half-

time of NADH was 53% shorter in Pgam2 (L38) mice than in NTg mice (*$p<0.05$ versus NTg; $n=4$ each; Figure 1B). First, we analyzed L22 and L38. Both transgenic lines survived normally over a follow-up period of 1 year. Both lines showed normal cardiac function, determined by echocardiography at rest (Table 1), and normal heart weights (Table 2). Thereafter, Pgam2 (L38), which showed the highest expression levels of the Pgam protein, was subjected to further analysis, and was designated as Pgam2 mice unless otherwise specified.

2. Myocardial uptake of ^{18}FDG or ^{125}I-9MPA was normal in Pgam2 mice.

To examine changes in substrate utilization in Pgam2 hearts, we examined the myocardial uptake of glucose and fatty acids using their analogs ^{18}FDG and ^{125}I-9MPA, respectively. The uptake of ^{18}FDG and ^{125}I-9MPA in Pgam2 mice was similar to that in NTg control mice (Figure 2A, Table S2).

3. Myocardial energy reserve assessed by in situ ^{31}P magnetic resonance spectroscopy (MRS) was normal in Pgam2 mice.

The energy reserve of the heart was analyzed by measuring high-energy phosphates using *in situ* ^{31}P magnetic resonance spectroscopy (MRS) [3]. The phosphocreatine (PCr)/βATP ratio, identified as a marker of myocardial energy reserve, was reported to be a prognostic indicator of heart failure [35]. The mean cardiac PCr/βATP ratio of NTg mice at rest was 2.0, which was consistent with a previous report [36]. The mean cardiac PCr/βATP ratio of Pgam2 mice at rest was not different from that of NTg mice (Figure 2B).

4. Metabolomic profile of Pgam2 mice.

To examine the effect of the persistent overexpression of Pgam2 on myocardial energy metabolism, we performed a comprehensive metabolomic analysis. The results of the quantification of

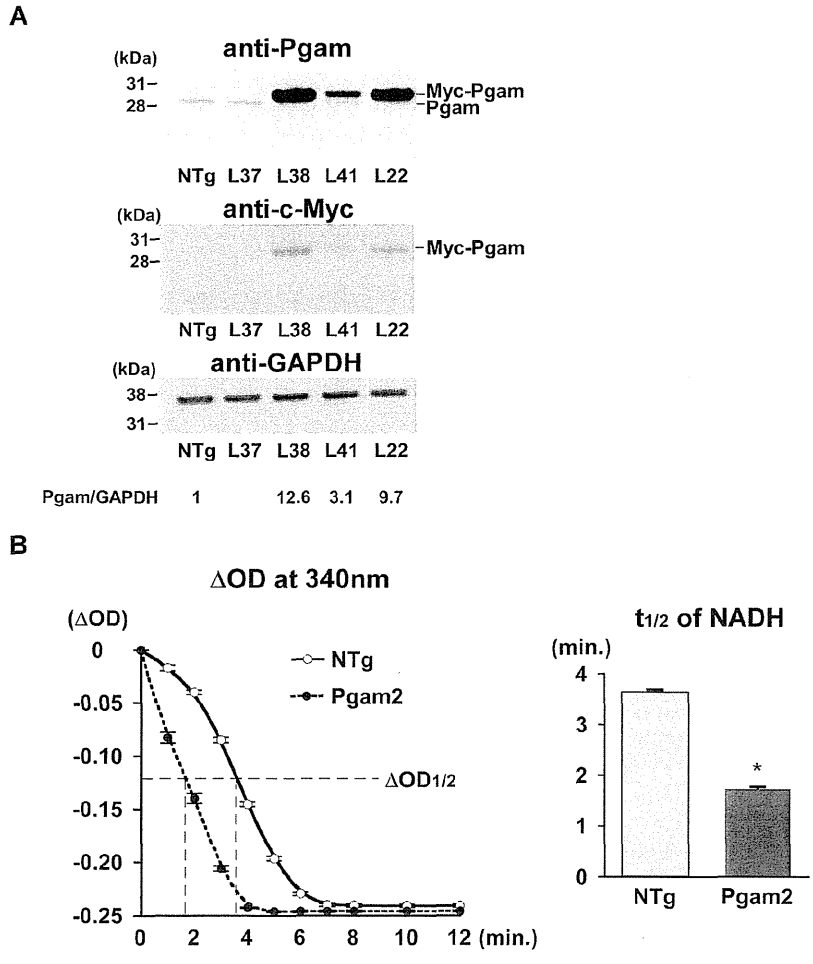

Figure 1. Generation of transgenic mice overexpressing Pgam2 in a heart-specific manner. (**A**) Transgenic mice overexpressing Pgam2 in a heart-specific manner were generated using the α-MHC promoter on a C57/BL6 background. The Pgam1 antibody (Abcam; Ab2220) detected both mouse PGAM1 and PGAM2 at similar sensitivities (Figure S1). Migration of the transgene product, the Pgam2 protein with a Myc-tag, was slower than that of the endogenous Pgam protein on a sodium dodecyl sulfate polyacrylamide gel electrophoresis (SDS-PAGE) gel. Two of the 3 lines of Pgam2 mice (line 22 (L22) and line 38 (L38)) expressed different total Pgam protein levels in the heart (9.7-fold and 12.6-fold, when measurements included endogenous Pgam relative to levels in non-transgenic (NTg) mice, respectively). (**B**) The enzymatic activity of phosphoglycerate mutase was analyzed via an NADH-consuming spectrophotometric assay. The vertical axis indicated differences in optical density (O.D.) at 340 nm from the value of the negative control without heart tissue lysate. The half-time of ΔO.D. at 340 nm was 53% lower in Pgam2 mice than in NTg mice ($n=4$ for each group).
doi:10.1371/journal.pone.0072173.g001

Table 1. Echocardiographic analysis of Pgam2 mice.

	NTg (n = 10)		Pgam2 (L22) (n = 10)		Pgam2 (L38) (n = 10)	
Heart rate (bpm)	545	± 13	533	± 14	541	± 9
LV diastolic diameter (mm)	3.62	± 0.05	3.89	± 0.04	3.44	± 0.04
LV systolic diameter (mm)	1.95	± 0.05	2.21	± 0.02	2.00	± 0.07
Fractional shortening (%)	44.7	± 0.7	43.2	± 2.9	41.9	± 1.9
Posterior wall thickness (mm)	0.67	± 0.06	0.53	± 0.01	0.67	± 0.07

Values are expressed as the mean ± SEM. NTg: non-transgenic mice; Pgam2: phosphoglycerate mutase 2 transgenic mice; bpm: beats per minute; LV: left ventricular.
doi:10.1371/journal.pone.0072173.t001

metabolites related to glycolysis and the TCA cycle, and amino acids and their derivatives, are listed in Table S3. Pgam2 overexpression significantly changed the metabolome of heart tissue (Figure 3 and Table S3). First, the levels of metabolites just upstream and downstream of Pgam were significantly changed, with 3-phosphoglycerate (3PG), 2-phosphoglycerate (2PG), and phosphoenolpyruvate (PEP) levels increasing, and 2,3-diphosphoglycerate (2,3-DPG) level decreasing. The levels of metabolites in the initial steps of the glycolytic pathway, such as glucose-6-phosphate (G6P), fructose-6-phosphate (F6P), and fructose-1,6-bisphosphate (F1,6BP), remained unchanged. Lactate, an end product of the glycolytic pathway, also did not change. Second, Pgam2 overexpression altered the levels of metabolites in the TCA cycle. The levels of metabolites in the first half of the TCA cycle were slightly higher, whereas acetyl-CoA and cis-aconitate were significantly higher. The levels of metabolites in the latter half of the cycle were slightly lower, whereas fumarate was significantly lower. Third, the levels of several amino acids and their derivatives were changed. For example, serine, betaine, the reduced-form glutathione (GSH), and aspartate decreased, while histidine, carnosine, and anserine increased.

5. Overexpression of Pgam2 suppressed the expression of genes related to glycolysis, and inhibited phosphofructokinase activity.

The overexpression of Pgam2 did not change the uptake of the glucose analogs, G6P and lactate, which indicated that the glycolytic flux may not be increased. Thus, we hypothesized that the persistent overexpression of Pgam2 may modify other enzymes in the glycolytic pathway. First, we examined the effect of Pgam2 overexpression on the gene expression of other rate-limiting glycolytic enzymes by quantitative real-time PCR. The gene expression levels of hexokinase 2, phosphofructokinase 1 (Pfk1), 6-phosphofructo-2-kinase/fructose-2,6-biphosphatase 1 (Pfkfb1), and 6-phosphofructo-2-kinase/fructose-2,6-biphosphatase 2 (Pfkfb2), the rate-limiting enzymes in glycolysis, were decreased (Figure 4A). The gene expression levels of hypoxia-inducible factor 1 α subunit (Hif-1α), a key transcription factor and positively regulates glycolytic enzymes [37], were decreased in Pgam2 mice. Since the increase in 3-phosphoglycerate, 2-phosphoglycerate, or phosphoenolpyruvate each resulted in the inhibition of phosphofructokinase [38], we measured the enzymatic activity of phosphofructokinase (PFK) using heart tissue lysates. The activity of PFK was significantly decreased in Pgam2 mice (Figure 4B). Thus, Pgam2 overexpression decreased the expression of genes related to glycolysis and PFK activity.

6. Overexpression of Pgam2 decreased the capacity for respiration and increased that for the generation of reactive oxygen species in vitro.

Since the levels of metabolites in the TCA cycle were changed and the function of the TCA cycle is closely linked to that of mitochondria, we examined the capacity for respiration and generation of reactive oxygen species (ROS) in mitochondria isolated from heart tissue. Oxygen consumption by isolated mitochondria measured *in vitro* was lower in Pgam2 mice (Figure 5A). The amount of H_2O_2 generated from isolated mitochondria measured *in vitro* was increased (Figure 5B). Thus, the regulation of respiration and ROS generation in mitochondria were impaired in Pgam2 mice.

7. Overexpression of Pgam2 suppressed the expression of genes related to mitochondria.

Since respiration and ROS generation were altered in isolated mitochondria, we quantified the expression of genes related to

Table 2. Pathological analysis of Pgam2 mice.

	NTg (n = 10)		Pgam2 (L22) (n = 10)		Pgam2 (L38) (n = 10)	
Body weight (BW, g)	25.2	± 0.6	25.6	± 0.8	24.4	± 0.4
Heart weight (HW, mg)	123.6	± 3.4	121.3	± 2.9	115.4	± 2.5
HW/BW (mg/g)	5.03	± 0.06	4.89	± 0.06	4.79	± 0.07
Lung weight (LW, mg)	151.2	± 2.8	150.7	± 2.5	154.0	± 3.8
LW/BW (mg/g)	6.22	± 0.11	5.87	± 0.09	6.29	± 0.11

Values are expressed as the mean ± SEM. NTg: non-transgenic mice; Pgam2: phosphoglycerate mutase 2 transgenic mice.
doi:10.1371/journal.pone.0072173.t002

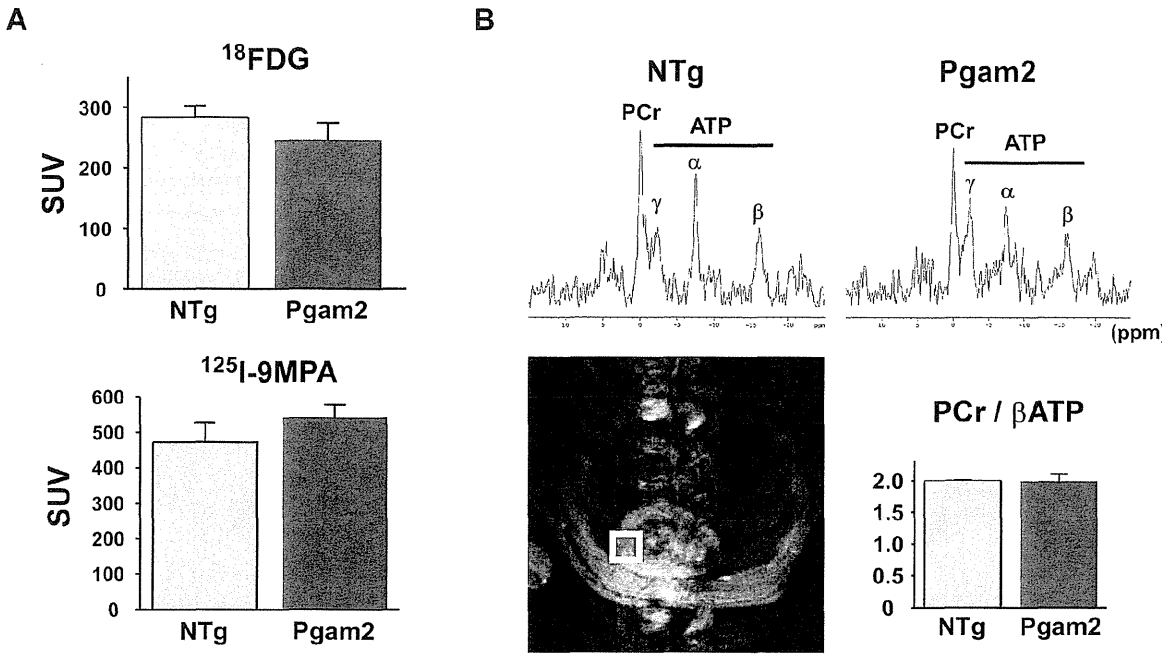

Figure 2. Myocardial substrate uptake and myocardial energy reserve were normal in Pgam2 mice. (**A**) Myocardial uptake of ^{18}F-deoxyglucose (^{18}FDG) and ^{125}I-15-(*p*-iodophenyl)-9-*R,S*-methylpentadecanoic acid (^{125}I-9MPA) did not differ from that in NTg mice (n = 13 for NTg and n = 18 for Pgam2 mice). SUV: standard uptake value. SUV = tissue concentration (MBq/g)/(injected dose (MBq)/body weight (g)). (**B**) Cardiac energy reserve was analyzed by measuring cardiac high-energy phosphates with *in situ* ^{31}P magnetic resonance spectroscopy (MRS). ^{1}H magnetic resonance (MR) imaging was used to define the region of interest to measure the ^{31}P MR spectrum of the anterior wall of the left ventricle (lower left panel). Representative *in situ* cardiac ^{31}P MR spectra from NTg and Pgam2 mice are shown (upper panel). ppm: parts per million. The cardiac phosphocreatine (PCr)/βATP ratio of Pgam2 mice at rest did not differ from that of NTg mice (NTg: n = 10; Pgam2 mice: n = 9; lower right panel).
doi:10.1371/journal.pone.0072173.g002

mitochondrial function. Peroxisome proliferator-activated receptor γ coactivator 1-α (PGC-1α) is a master regulator of mitochondrial function and biogenesis, and regulates the expression of peroxisome proliferator-activated receptor α (PPARα) and PPARδ, estrogen-related receptor α (ERRα), nuclear respiratory factor-1 (NRF-1), and mitochondrial transcription factor A (Tfam). The gene expression levels of PPARα decreased, accompanied by a decrease in enzymes involved in fatty acid metabolism, such as carnitine palmitoyltransferase-1b (CPT-1b) and isocitrate dehydrogenase (IDH3α) (Figure 6A, 6B). The gene expression levels of ERRα, PPARδ, and Tfam also decreased (Figure 6A). The gene expression levels of enzymes in the TCA cycle, such as oxoglutarate dehydrogenase (OgDh) and succinyl-CoA synthetase (SCS), were decreased (Figure 6C), and this decrease may explain the accumulation of TCA cycle metabolites, such as acetyl-CoA and cis-aconitate. The expression levels of genes in the mitochondrial respiratory chain, such as mitochondrially encoded NADH dehydrogenase 4 (ND4), alpha-subcomplex 9 of complex I (α-S9), succinate dehydrogenase b (SDHB), iron-sulfur protein (Fe-S), cytochrome b (Cyt-b), cytochrome c (Cyt-c), and mitochondrial cytochrome c oxidase subunit VIIa 1 (Cox7a1), were decreased. The gene expression levels of uncoupling protein (UCP) 2, UCP3, and manganese superoxide dismutase (MnSOD) were also decreased (Figure 6D).

8. Mitochondrial morphology and a marker of ROS in vivo were normal in Pgam2 mice.

A light microscopic examination revealed that no cardiomyopathic changes, such as necrosis or fibrosis, were observed in Pgam2 mice (data not shown). Electron-microscopic analysis showed no apparent abnormalities. The size and number of mitochondria did not differ between Pgam2 (H) mice and their NTg littermates. Neither the degeneration nor collapse of mitochondria was observed (Figure S2A). We then measured TBARS levels, a marker of lipid peroxidation, in heart tissue. TBARS levels were normal in the heart tissue of Pgam2 mice (Figure S2B), which indicated that ROS generation was not increased *in vivo* at the baseline.

9. Cardiac function in response to dobutamine was impaired in Pgam2 mice.

As described, cardiac function at rest as assessed by echocardiography was normal in Pgam2 mice. However, the expression levels of genes related to mitochondrial function were decreased and the capacity of mitochondrial function assessed *in vitro* was perturbed in Pgam2 mice. Since the decrease in gene expression levels related to mitochondrial function was previously shown to be associated with the decrease in contractile reserve under dobutamine infusion [39], we assessed cardiac function using cardiac catheterization under graded doses of dobutamine infusion. The change in maximum dP/dt, a marker of cardiac systolic function, in response to dobutamine was blunted in Pgam2 mice (Figure 7A, 7B).

10. Pgam2 mice developed systolic dysfunction and myocardial fibrosis in response to pressure overload.

To further examine the cardiac function of Pgam2 mice under stress conditions, we examined the effect of Pgam2 overexpression

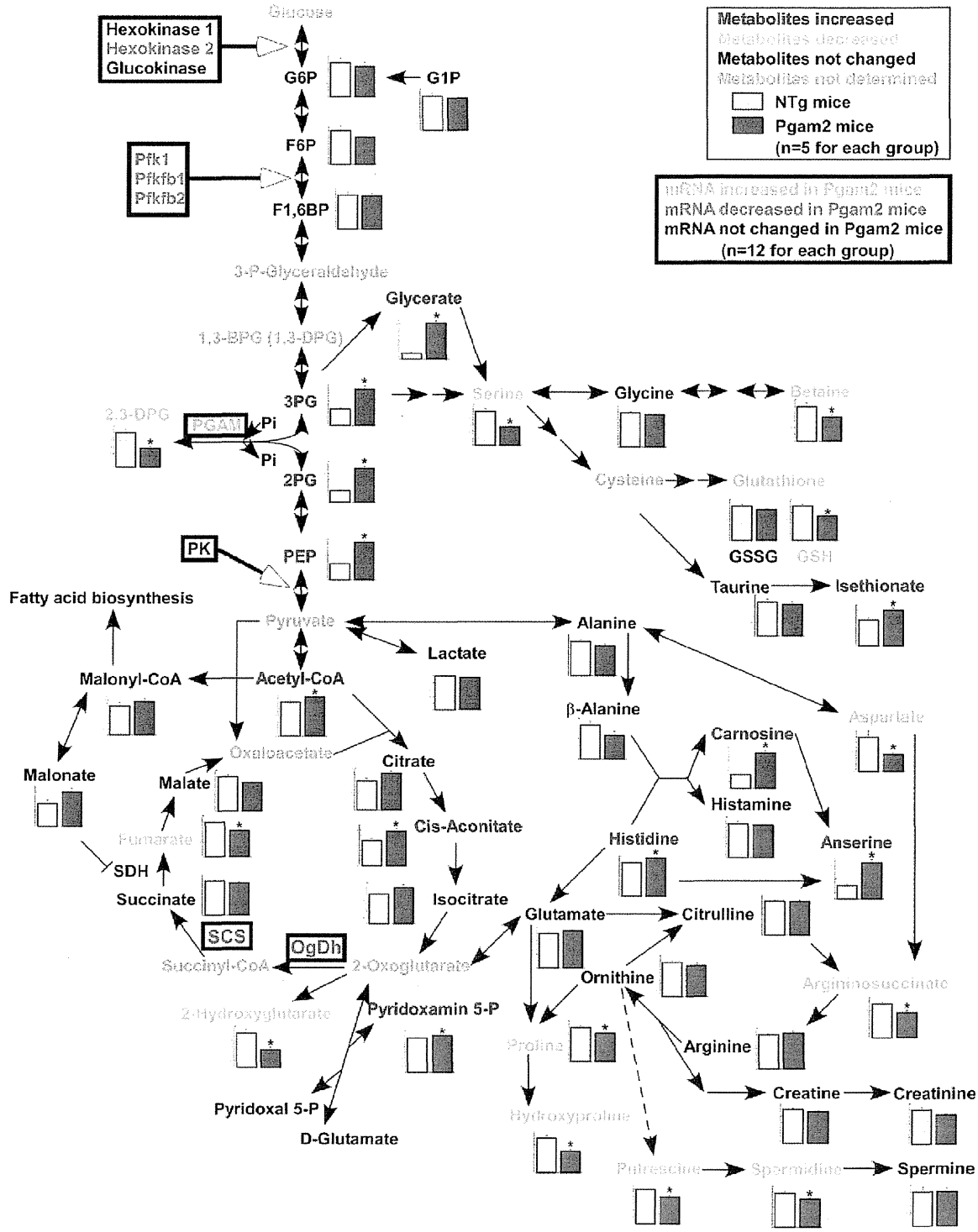

Figure 3. Metabolomic analysis revealed an alteration in the intermediates of glycolysis, the TCA cycle, and amino acids. Comprehensive metabolomic analysis revealed that levels of the upstream metabolites of phosphoglycerate mutase remained unchanged, while levels of the downstream metabolites, such as 2-phosphoglycerate and phosphoenolpyruvate, were increased. Lactate, the final metabolite of glycolysis, also remained unchanged. While metabolites of the first half of the TCA cycle, such as acetyl-CoA and cis-aconitate, were increased, those of the latter half, such as fumarate, were decreased (n = 5 for each group). The expressions of some genes involved in glycolysis and the TCA cycle, which are shown in Figure 4 or Figure 6, are also presented.
doi:10.1371/journal.pone.0072173.g003

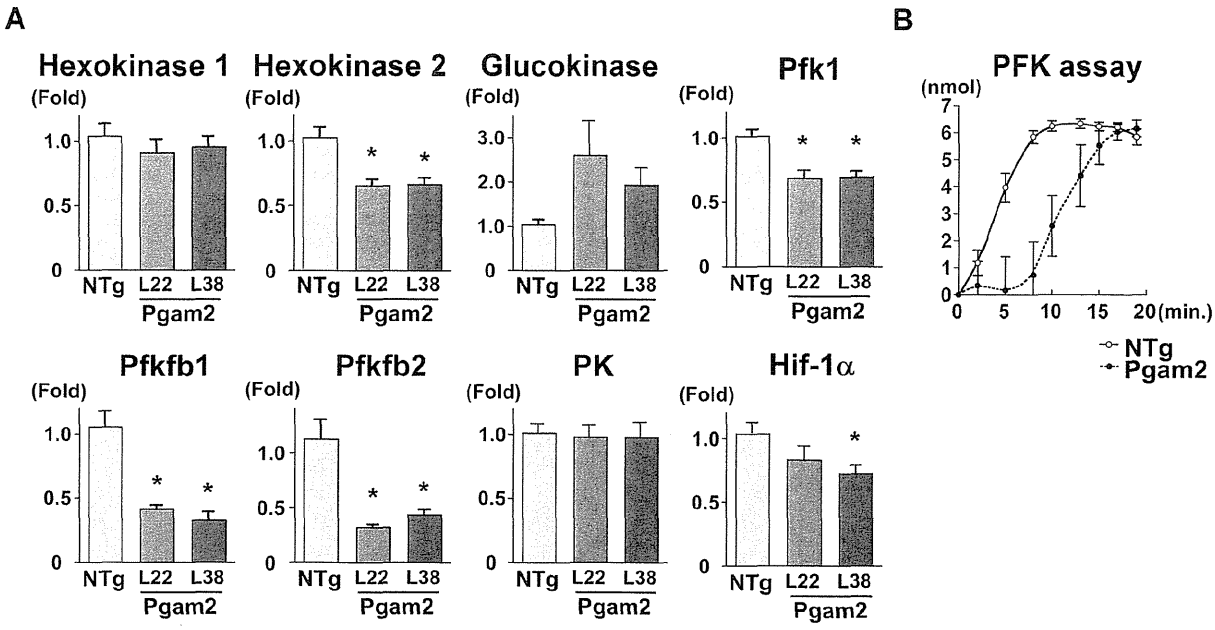

Figure 4. The expression of genes related to glycolysis and phosphofructokinase (PFK) enzymatic activity were modified. (**A**) The expression of genes related to glycolysis was analyzed using quantitative real-time PCR. Hexokinase 2, 6-phosphofructo-2-kinase/fructose-2,6-biphosphatase 1 (Pfkfb1), 6-phosphofructo-2-kinase/fructose-2,6-biphosphatase 2 (Pfkfb2), and phosphofructokinase 1 (Pfk1) levels were decreased in Pgam2 mice. The amount of target gene mRNA was normalized by 18S rRNA mRNA. Values are the mean ± SEM. Gene expression levels in Pgam2 mice were compared with those of NTg mice. *$p<0.05$ versus NTg mice ($n=12$ for each group). (**B**) Measuring PFK enzymatic activity. Pgam2 overexpression inhibited myocardial PFK activity. The vertical axis indicated the amount of NADH produced, which represented PFK activity (NTg: $n=6$, Pgam2 mice: $n=5$).
doi:10.1371/journal.pone.0072173.g004

on pressure overload. NTg or Pgam2 mice were subjected to transverse aortic constriction (TAC) or a sham operation at 3 months of age, and were analyzed 14 days after the operation. Pgam protein levels in NTg mice with TAC were not different from those in NTg mice with the sham operation (Figure 8 and Table 3). Pgam protein levels in Pgam2 mice with TAC were 6.9-fold higher than those in NTg mice with TAC.

The systolic function of the heart, as assessed by fractional shortening (FS), was normal in NTg mice and Pgam2 mice with the sham operation. Upon TAC, NTg mice developed cardiac hypertrophy with preserved systolic function. However, Pgam2 mice with TAC developed systolic dysfunction (Figure 9A). The heart weight/body weight ratio (HW/BW) of Pgam2 mice was higher than that of NTg mice with TAC (Figure 9B). The lung

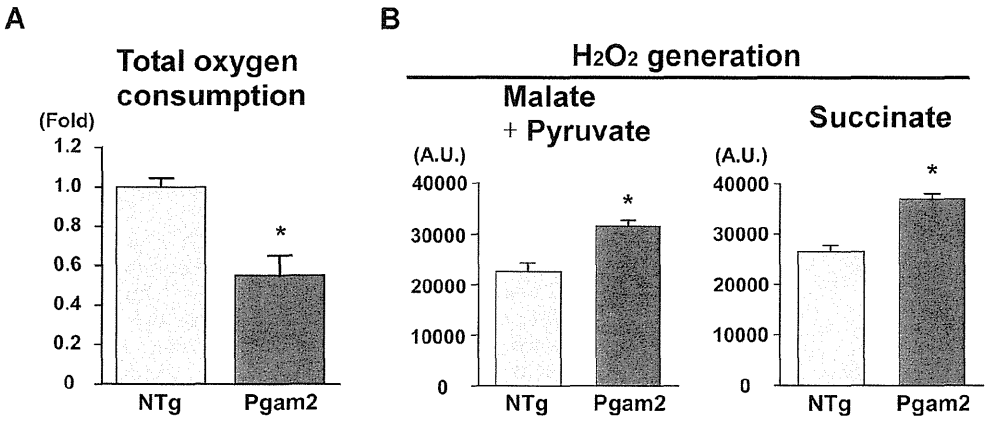

Figure 5. Respiration was decreased and ROS production was increased in the isolated mitochondria of Pgam2 mice. (**A**) Oxygen consumption in isolated mitochondria was measured using an oxygen electrode cuvette. Total oxygen consumption was lower in Pgam2 mice. Values are the mean ± SEM. *$p<0.05$ versus NTg mice (NTg: $n=3$; Pgam2 mice: $n=5$). (**B**) Generation of H_2O_2 by isolated mitochondria. Malate and pyruvate, or succinate, were used as substrates. The generation of H_2O_2 increased in Pgam2 mice both with malate + pyruvate and with succinate. Values are the mean ± SEM. *$p<0.05$ versus NTg mice ($n=6$ for each group). A.U.: arbitrary unit.
doi:10.1371/journal.pone.0072173.g005